이학박사학위논문

microRNA-9-3p의 해마에서의 시냅스 가소성과 기억에 미치는 영향에 대한 연구

Studies on the role of microRNA-9-3p in hippocampal synaptic plasticity and memory

2016년 8월

서울대학교 대학원

뇌인지과학과

심 수 언

ABSTRACT

Studies on the role of microRNA-9-3p in hippocampal synaptic plasticity and memory

Su-Eon Sim

Department of Brain and Cognitive Sciences

The Graduate School

Seoul National University

MicroRNAs (miRNAs) are small noncoding RNAs (~22 nt) that post-transcriptionally regulate gene expression in many tissues. Post-transcriptional gene regulation through miRNAs is thought to play essential roles in the physiological function of brain including synaptic plasticity and memory. Although a number of brain-enriched miRNAs are identified, only a few specific miRNAs have been reported as a critical regulator of learning and memory. miR-9-5p/3p are evolutionarily conserved, brain-enriched microRNAs known to regulate development and their changes have been implicated in several neurological disorders, yet their role in mature neurons is largely unknown. Here I reveal the roles of miR-9-3p (or miR-9*) in the hippocampal synaptic plasticity and memory, using miRNA sponge, a competitive inhibitor of miRNA. Whole-cell recording showed

that inhibition of miR-9-3p, but not miR-9-5p impaired long-term potentiation (LTP) in the hippocampal Shaffer collateral-CA1 (SC-CA1) synapses without affecting basal synaptic transmission and membrane excitability. Moreover, inhibition of miR-9-3p in the hippocampus resulted in learning and memory deficits in Morris water maze, object location memory task and trace fear conditioning. These results suggest that miR-9-3p-mediated regulation has important roles in synaptic plasticity and hippocampus-dependent memory. Furthermore, I identified 7 candidate target genes of miR-9-3p by a series of bioinformatics analysis and comprehensive literature search, and validated these putative candidate genes were regulated by miR-9-3p. Finally, I found out the protein level of two putative candidate genes, *Dmd* and *SAP97*, was actually increased in the CA1 tissue expressing the miR-9-3p sponge, proposing the molecular mechanism of miR-9-3p.

In summary, I found that miR-9-3p, but not miR-9-5p, has an important role in hippocampal LTP and memory. Moreover, I identified *in vivo* binding targets of miR-9-3p, *Dmd and SAP97*, which have a crucial role in LTP. This study provides the very first evidence for the critical role of miR-9-3p in synaptic plasticity and memory in the adult mouse.

.....

Key words: microRNA, miR-9-5p/3p, hippocampus, synaptic plasticity, memory

Contents

LIST OF FIGURES and TABLES

CHAPTER 1. INTRODUCTION

BACKGROUND

What is a microRNA?

microRNAs (miRNAs) comprise small (~22-nucleotide) non-coding RNAs regulating the stability and translation of target mRNAs via complementary binding to 3' untranslated regions (3' UTRs). miRNAs are known to fine-tune the expression of various target genes and orchestrate diverse biological processes including proliferation, development, metabolism, apoptosis and cell fate decision (Bartel, 2004; He and Hannon, 2004). It is predicted that miRNAs regulate 30~60 % of all protein-coding genes of mammals (Friedman et al., 2009; Lewis et al., 2005)

The very first evidences of miRNA were suggested by two monumental papers published in 1993 (Lee et al., 1993; Wightman et al., 1993). The authors discovered a small non-coding RNA of *Caenorhabditis elegans*, *lin-4*, suppresses the expression of *lin-14* without affecting the level of *lin-14* mRNA. The authors also found that 3' UTR of *lin-14* includes multiple complementary elements to *lin-4* and is necessary and sufficient to *lin-4*-mediated suppression. Seven years later, another non-coding small regulatory RNA of *C. elegans*, *let-7*, was discovered (Reinhart et al., 2000). The *lin-4* and *let-7* RNAs were called as small temporal RNAs (stRNAs) because of their similar role to coordinate developmental timing. But the term of stRNA was not used widely, since less than one year later, the term of ‘microRNA’ was introduced. Three labs cloned about one hundred small RNAs from flies, worms and human and referred to them as microRNA (Lagos-Quintana et al., 2001; Lau et al., 2001; Lee and Ambros, 2001). After the pioneers identified the class of small regulatory RNAs as microRNA, researchers started to reveal

hundreds of additional miRNA genes from animals, plants and viruses (Berezikov et al., 2006). Based on miRBase 21 database released in 2014, the number of miRNAs reaches 2588 and 1915 mature miRNAs in human and mouse, respectively.

The biogenesis of microRNA

Transcription of miRNAs, generally by RNA polymerase II (Pol II), produces long primary miRNAs (pri-miRNAs) which fold into a stemloop structures containing imperfectly base paired stems (Lee et al., 2004). A single pri-miRNA can contain several different miRNAs (Lee et al., 2002). Pri-miRNAs are cleaved within the nucleus by the microprocessor complex which consist of RNase III enzyme Drosha and the double-stranded RNA-binding domain protein DGCR8 (Denli et al., 2004; Han et al., 2004; Lee et al., 2003). This process generates a precursor miRNAs (pre-miRNAs) which form a ~70-nucleotide single hairpin. These pre-miRNAs are exported to the cytoplasm by Exportin 5 transporter via a Ran-GFP-dependent mechanism (Bohnsack et al., 2004; Yi et al., 2003), and further processed by another RNase III enzyme Dicer to ~23-nucleotide miRNA duplexes. Usually, only one strand is selected and loaded into the RNA-induced silencing complex (RISC) and function as mature miRNA, while the other strand is degraded (Schwarz et al., 2003). After incorporated into RISC, the mature miRNA bind to 3' UTR of target mRNAs by base-pairing interaction, which results in translational repression and/or mRNA destabilization (Martinez and Tuschl, 2004).

microRNAs in synaptic plasticity and memory

In the nervous system, there are multiple evidences suggesting miRNAs

play essential roles in synaptic plasticity and memory which require complex and dynamic regulation of gene expression (Schratt, 2009). Adult forebrain-specific disruption of *Dicer1*, a key RNase III enzyme for miRNAs biogenesis, results in decreased expression level of a set of brain-specific miRNAs, inducing improved learning and memory in various behavioral tasks such as Morris water maze, place preference test and trace fear conditioning (Konopka et al., 2010). The brain-specific miRNA, miR-134, regulates the size of dendritic spines, excitatory synaptic transmission and synaptic plasticity (Gao et al., 2010; Schratt et al., 2006). In visual cortex, miR-132 is induced by visual stimulation and has a crucial roles in the plasticity of visual cortex circuit and ocular dominance (Mellios et al., 2011; Tognini et al., 2011). The induction of miR-132 is regulated by cAMP response element binding protein (CREB) which is a crucial stimulus induced transcription factor regulating many fast-response genes and playing a key role in dendritic development and synaptic plasticity (Klein et al., 2007). The role of another brain-specific miRNA, miR-124, was studied in *Aplysia californica*. It is exclusively expressed in the sensory neuron compared to the motor neuron and regulates serotonin-mediated synaptic plasticity through the regulation of CREB (Rajasethupathy et al., 2009).

miR-9-5p/3p

A single miR-9 precursor produces two mature miRNAs, miR-9-5p and miR-9-3p (Fig. 1). While most mature miRNAs are preferentially produced from only one strand, the *miR-9* gene produce two mature miRNAs from either 5' arm (miR-9-5p) or 3' arm (miR-9-3p).

miR-9-5p/3p is evolutionarily highly conserved across vertebrate species

(Fig. 2) and ancient in evolution. The *miR-9* gene emerged at the transition towards triploblasty and most vertebrate species have several copies of this gene (Coolen et al., 2015). *Drosophila* has 5 genes corresponding to miR-9-5p/3p and drosophila *miR-9a* gene is identical to the one in human (Wheeler et al., 2009). Furthermore, the seed sequence of miR-9-3p is identical to that of the invertebrate-specific miRNAs, miR-4 and miR-79, which implies the functional importance of miR-9-5p/3p (Lai et al., 2004).

Many studies revealed tissue specific miRNAs using various detection method such as tissue-specific cloning and northern blotting (Lagos-Quintana et al., 2002; Sempere et al., 2004), *in situ* detection using locked nucleic acid (LNA) probes (Kapsimali et al., 2007; Kloosterman et al., 2006), microarray (Miska et al., 2004), RNA library sequencing (Landgraf et al., 2007) and cell type specific sequencing (He et al., 2012). Through these studies, miR-9-5p/3p have been defined as brain-specific miRNAs.

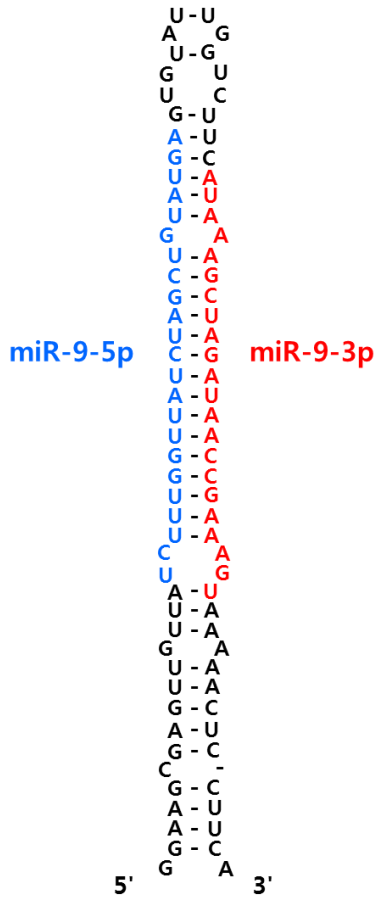

mmu-miR-9-2 precursor

Figure 1. Stem loop structure of mouse miR-9 precursor

miR-9-5p sequence is in blue and miR-9-3p sequences is in red. There are three genetic loci encoding miR-9-5p/3p in mammals: miR-9-1, miR-9-2 and miR-9-3. This diagram shows pre-miRNA of miR-9-2 locus.

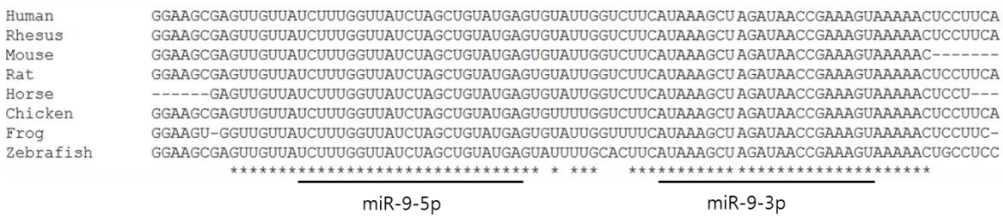

Figure 2. Evolutionally conserved nucleotide sequence of miR-9 precursor in vertebrate

Alignment of pre-miR-9 sequences from various vertebrates. Sequences are obtained from miRBase (Kozomara and Griffiths-Jones, 2014) (http://www.mirbase.org/). Multiple Sequence Alignment (MSA) tool in European Bioinformatics Institute (EMBL-EBI) was used for alignment of sequences (http://www.ebi.ac.uk/Tools/msa/).

Previous functional studies about miR-9-5p/3p

Because *miR-9-5p/3p gene* is one of the most abundant brain-specific miRNA, many neuroscientists have investigated the role of miR-9-5p/3p in neuron. However, most of the studies of miR-9-5p/3p have focused on their developmental role, even though miR-9-5p/3p is highly expressed in both developing and adult brain.

miR-9-5p/3p was shown to be involved in neurogenesis (Krichevsky et al., 2006; Leucht et al., 2008; Shibata et al., 2011), proliferation and differentiation of neural progenitor cell (Delaloy et al., 2010; Zhao et al., 2009) and axon development (Dajas-Bailador et al., 2012; Otaegi et al., 2011). Overexpression of miR-9-5p/3p in the zebrafish and mouse embryo induced the reduction of the number of neural progenitor cells (Leucht et al., 2008; Zhao et al., 2009). Moreover, loss-of-function of miR-9-5p/3p led the increase of proliferation of neural progenitor cells (Coolen et al., 2012; Shibata et al., 2011). These results proposed that miR-9-5p/3p negatively regulates proliferation of neural progenitor cells. However, the opposite role was shown in human embryonic stem cell-derived neural progenitor (Delaloy et al., 2010), which implies that the role of miR-9-5p/3p can be diverse depend on different context.

The miR-9-3p alone was also suggested to be involved in neural development (Wei et al., 2013; Yoo et al., 2009; Yoo et al., 2011). miR-9-3p was shown to control the transition from neural progenitor to post-mitotic neurons by switching the chromatin remodeling complexes from neural-progenitor-specific BAF (npBAF) to neuron-specific BAF. Furthermore, suppressing miR-9-3p activity in post-mitotic neurons induced the expression of BAF53a which is an npBAF (Yoo

et al., 2009; Yoo et al., 2011), suggesting that miR-9-3p is critical for neuronal differentiation. Moreover, the expression levels of miR-9-3p are decreased in neurodegenerative diseases such as Huntington's and Alzheimer's disease (Cogswell et al., 2008; Packer et al., 2008).

PURPOSE OF THIS STUDY

After the miRNA family was discovered and classified, scientists have enthusiastically investigated miRNAs for 15 years. By these efforts, many secretes of this powerful regulatory RNA family have been revealed, but plenty of questions were still remained to be solved. miR-9-5p/3p was discovered in early stage of miRNA research and attracted the attention of neurobiologists due to its brain-specific expression. However, most of functional studies have focused on their role in neuronal development, despite of the abundant expression of miR-9-5p/3p in post-mitotic neurons. In this study, I will investigate the function of miR-9-5p/3p in adult brain, especially, related with hippocampal synaptic plasticity and memory.

In chapter II, the effects of inhibition of miR-9-5p/3p activity on hippocampal synaptic plasticity and memory are examined. First, I establish miRNA sponge system and verify its efficacy to inhibit the activity of endogenous miR-9-5p or miR-9-3p. Next, the role of miR-9-5p/3p in synaptic plasticity and synaptic transmission was tested using whole cell patch recording technique. Finally, I test any behavioral changes induced by miR-9-3p inhibition. Three different behavior assays are used for examining hippocampus-dependent memory.

In chapter III, the molecular target of miR-9-3p is investigated. Based on the general role of miRNA, miR-9-3p should regulate translation of a set of genes. To find putative candidates, I perform a series of bioinformatics analysis and find a set of genes whose 3' UTR can be regulated by miR-9-3p. Finally, I find a novel target gene of miR-9-3p, examining whether protein level of candidate gene is regulated by miR-9-3p mediated by evolutionally conserved target sequences of

miR-9-3p within 3' UTRs.

CHAPTER 2.

Role of miR-9-3p in the hippocampal synaptic plasticity and memory

INTRODUCTION

The hippocampus is considered as a crucial brain system responsible for the formation of new episodic memories and spatial memory. The famous case of patient H.M. whose both temporal lobes including hippocampi are surgically removed reported that the loss of hippocampus impaired the ability to acquire new episodic memory and induced a partial loss of old episodic memories, while vocabulary, short-term memory and procedural learning were intact (Milner et al., 1998; Scoville and Milner, 1957). Another role of hippocampus is related with spatial memory and navigation. Single-unit recording in freely moving rodents reveled that hippocampal neurons fire when animals move in a particular location of the environment, which represents the responsiveness of hippocampus to spatial information. These hippocampal cells encoding spatial information are referred as ‘place cells’ (O'Keefe and Dostrovsky, 1971). Based on these features of hippocampus, the several behavior tasks were development to access hippocampus-dependent spatial memory. Morris water maze, for example, animal have to remember spatial cues to escape by finding a small hidden platform. The animals which have lesions in hippocampus failed to find the location of hidden platform (Morris et al., 1982).

The formation of memory requires a delicate and complicate process widely considered a long-term change of synaptic function, synaptic plasticity (Kandel, 2012; Malinow and Malenka, 2002; Martin et al., 2000). Tim Bliss and Terje Lømo first discovered the phenomenon of strong activity-induced long lasting change of synaptic responsiveness in hippocampus, later referred as long-term

potentiation (LTP) (Bliss and Lømo, 1973). Especially, the enhancement of synaptic strength in hippocampal SC-CA1 synapses, hippocampal LTP, is thought to be a key process to establish hippocampus-dependent memory, which requires numerous signaling pathways and *de novo* protein synthesis (Bliss and Collingridge, 1993; Lynch, 2004; Sutton and Schuman, 2006). A vast body of evidence showed that impaired LTP in hippocampus CA1 region is accompanied with poor performance in hippocampus-dependent behavior tasks, which implies an intimate relationship between hippocampal LTP and hippocampus-dependent memory formation (Atkins et al., 1998; Giese et al., 1998; Tsien et al., 1996).

In present study, I investigated the role of miR-9-5p/3p in hippocampus which is a well-established experimental model to examine synaptic plasticity and memory. The activity of miR-9-5p/3p was inhibited by miRNA-sponge system in hippocampus, and its effect on synaptic plasticity and basal synaptic transmission was examined by whole cell patch recording. In addition, three different behavior test was performed to test the effect of miR-9-3p inhibition on hippocampal dependent memory.

EXPERIMENTAL PROCEDURES

Animals

Male C57BL/6N mice were used for all experiments. The electrophysiology and behavioral experiments utilized 4~5-week-old and 8-week-old mice, respectively, purchased from Orient Bio. Inc. Korea. Animals were housed on a 12/12 h light/dark cycle in standard laboratory cages with access to food and water ad libitum. Mice were cared for in accordance with the regulation and guidelines of Institutional Animal Care and Use Committees (IACUC) of Seoul National University.

Construction of sponge plasmid and AAV production

Oligonucleotides (Integrated DNA Technologies) containing 6 bulged binding sites for miR-9-3p and 7 bulged binding sites for miR-9-5p were subcloned into pEGFP-C1 with BglII and HinDIII. EGFP-miR-9-3p and EGFP-miR-9-5p sponge was subcloned into an AAV vector with the human synapsin promoter (hSYN) using NheI and HindIII. For the EGFP-CXCR4 control sponge, a CMV-d2EGFP-CXCR4 plasmid was purchased from Addgene (plasmid 21967) and subcloned into a pEGFP-C1 vector and then an AAV vector, in the same manner as the EGFP-miR-9-3p sponge. The EGFP-CXCR4 control sponge has 7 bulged binding sites for artificial microRNA based on a sequence from the CXCR4 gene. AAVs expressing each sponge were produced as described previously (Choi et al., 2014). Briefly, human embryonic kidney (HEK)-293T cells were transfected with an AAV vector expressing each sponge, AAV2/1, and pAdDeltaF6 using calcium phosphate. AAVs were harvested and purified using an iodixanol (Axis-Shield) gradient.

Stereotaxic virus injection

Mice were deeply anesthetized with a ketamine/xylazine mixture and mounted in a stereotaxic apparatus (Stoelting Co.). Their eyes were protected by ophthalmic gel. The virus was injected using a 33-gauge metal needle (Plastic One) connected to a 10-μl Hamilton syringe (Hamilton Co.) at a rate of 0.1 μl/min. After the injection, the needle was left for an additional 7 min before withdrawal. For 3-week-old male mice, 0.5 μl of virus was injected into the CA1 (stereotaxic coordinates: -1.9 mm anteroposterior [AP], ± 1.25mm mediolateral [ML], -1.5 mm dorsovental [DV]). For 8-week-old mice, I targeted two sites in the CA1 of both hippocampi and injected 0.5 μl of virus into each site (site one: -1.6 mm [AP], ±1.3 mm [ML], -1.6 mm [DV]; site two: -2.3 [AP], ±2.0 mm [ML], -1.7 mm [DV]).

Immunohistochemistry

The AAV-miR-9-3p or AAV-control sponge infused mice were perfused with 4% paraformaldehyde (PFA) in PBS. The brains were removed and kept in 4% PFA overnight at 4℃. Brains were sectioned with a cryostat at a thickness of 40 μm. Sections were incubated in a blocking solution (2% goat serum, 0.2% Triton X-100, in PBS) for 1 h and then incubated with the NeuN (1:1000, Millipore) antibody in the blocking solution overnight at 4℃. Sections were then incubated with anti-mouse Alexa Fluor 555 IgG (1:300, Invitrogen) in blocking solution for 2 h at RT. Sections were then imaged with a fluorescent microscope (IX51; Olympus).

Electrophysiology

Animals (4~5-week-old male mice) were deeply anesthetized with isoflurane, decapitated, and coronal hippocampal slices (300-μm thick) were prepared using a vibratome (VT1200S; Leica). Slices were allowed to recover for at least 1 h in a recovery chamber at room temperature (RT) with oxygenated artificial cerebrospinal fluid (ACSF) containing (in mM) 124 NaCl, 2.5 KCl, 1 NaH2PO4, 25 NaHCO3, 10 glucose, 2 CaCl2, and 2 MgSO4. After recovery, the CA3 region was removed from the slice; the remaining hippocampal tissue was transferred to a recording chamber and maintained at RT with oxygenated ACSF. For experiments that examine LTP and basal synaptic properties, the recording pipettes (3~5 MΩ) were filled with an internal solution containing (in mM) 145 K-gluconate, 5 NaCl, 10 HEPES, 1 MgCl2, 0.2 EGTA, 2 MgATP, and 0.1 Na3GTP (280~300 mOsm, adjust to pH 7.2 with KOH). Picrotoxin (100 μM) was added to the ACSF to block the GABA-R-mediated currents. EPSCs were evoked at 0.05 Hz and three successive EPSCs were averaged and expressed relative to the normalized baseline. Since the LTP was measured by using whole-cell recording, the baseline responses were recorded only for 5 min to minimize the washout effect. To induce theta-burst LTP, theta-burst stimulation (TBS), 5 trains of burst with 4 pulses at 100 Hz, at a 200-ms interval were repeated 4 times at 10-s intervals. For experiments measuring LTD and NMDAR-mediated currents, following internal solution was used (in mM): 130 $CsMeSO_4$, 5 NaCl, 10 HEPES, 1 $MgCl_2$, 0.5 EGTA, 4 MgATP, 0.3 Na_3GTP, 5 QX-314 (280~300 mOsm, adjust to pH 7.2 with CsOH). LTD was induced with a 1 Hz, 5 min train at -40 mV in the presence of picrotoxin (100μM). To measure NMDAR-mediated currents, CNQX (20μM) and picrotoxin (100μM) were added to the ACSF. Input-output

relationship of NMDA receptor-mediated EPSC was recorded at -30 mV. Experiments measuring mEPSC and sEPSC were performed with the following internal solution (in mM) 100 Cs-gluconate, 5 NaCl, 10 HEPES, 10 EGTA, 20 TEA-Cl, 3 QX-314, 4 MgATP, and 0.3 Na3GTP (280~300 mOsm, pH adjusted to 7.2 with CsOH). Both mEPSC and sEPSC were recorded in the presence of picrotoxin (100 μM). For the mIPSC and sIPSC recordings, I used the following internal solution (in mM) 145 KCl, 5 NaCl, 10 HEPES, 10 EGTA, 10 QX-314, 4 MgATP, and 0.3 Na3GTP (280~300 mOsm pH adjusted to 7.2 with KOH). Both mIPSC and sIPSC were recorded in the presence of kynurenic acid (2 μM). For the mEPSC and mIPSC recordings, 1 μM tetrodotoxin was added. Hippocampal neurons were voltage-clamped at -70 mV using an Axopatch 200B (Molecular Devices). Only cells with a change in access resistance <20% were included in the analysis. AAV-GFP-sponge expression was confirmed by a cooled CCD camera (ProgRes MF cool; Jenoptik) and fluorescence microscope (BX51WI; Olympus). MiniAnalysis program (Synaptosoft) was used for mEPSC, sEPSC, mIPSC, and sIPSC analysis.

Morris water maze

The water maze was made of an opaque grey Plexiglas, 140 cm in diameter and 100 cm in height. The maze was filled with water (22~23℃) to a depth of 30 cm. The water was kept opaque by adding a small amount of white paint. The hidden platform (a circle, 10 cm in diameter) was placed at the center of the target quadrant and submerged approximately 1.5 cm below the surface of the water. For acquisition of spatial memory, mice were placed in water and trained to find the hidden platform. The training consisted of four 60-s trials per day for five consecutive days. The

starting point was randomized for the four trials so that they were equally distributed among the four maze quadrants. If the mice failed to find the platform within 60 s, they were guided manually to the platform by an experimenter and allowed to remain on the platform for 20 s. When the mice found and mounted on the platform, they were allowed to remain on the platform for 20 s. The inter-trial interval (ITI) was 60 s between trials. The probe trial was performed on day 6 to measure spatial memory, which consisted of free-swimming (60 s) without the platform. For the probe test, mice were placed in the center of the maze.

Object location memory task

The object location memory task was performed as previously described (Lee et al., 2014). All experiments were performed under dim light. Each mouse was handled for 5 min per day for 4 consecutive days. For habituation, mice were exposed to the arena, an acrylic box (33 × 33 × 30 cm), for 15 min for 2 days without the objects. A black triangle shaped sticker was placed on one side of the arena to provide a visual anchor. During the training session, mice were allowed to explore two identical objects for 10 min. For the test session, 24 h after training, one of the objects was placed at the same location as the training session (non-displaced object), but the other was moved to a new location (displaced object), and then mice were placed back into the arena for 5 min. Switching the placement of the objects was randomly counterbalanced. Training and test sessions of the task were recorded with a digital camera placed above the arena. The exploration time was manually counted to be the amount of time the mice spent sniffing or exploring the object within 1 cm of the object. The discrimination index was calculated as ([displaced object exploration

time/total object exploration time] * 100). All sessions of the task and analysis were performed blindly. Mice that showed more than 65% preference for any object during the training session were excluded from the analysis.

Trace fear conditioning

Trace fear conditioning was performed as previously described (Lim et al., 2014). White noise (15 s, 3 kHz, 75 dB) was used as the conditioned stimulus (CS) and a scrambled foot shock (0.5 s, 0.5 mA) was used as the unconditioned stimulus (US). For trace training, mice were exposed to the conditioning chamber for 60 s and subjected to 7 CS-trace-US-ITI trials (trace, 30 s; ITI, 210 s). The next day, mice were exposed to the novel context, which was changed to octagonal walls, a different grid, vanilla scent, and red light. The memory test consisted of a 60 s acclimation period followed by seven CS-ITI trials (ITI, 210 s). All behavioral tests were performed in the conventional conditioning chamber and analyzed by the FreezeFrame system (Coulbourn Instruments).

Open field task

Mice were allowed to explore the arena, an opaque white box (40 × 40 × 40 cm), under dim light. The movement of each mouse in the central (within a 20 × 20 cm) and peripheral area was recorded for 10 min. All data were recorded and analyzed with EthoVision 3.1 (Noldus).

Elevated zero maze task

The elevated zero maze is a modified version of the elevated plus maze. The elevated zero maze avoids the ambiguity of time spent in the central square of the elevated plus maze. The maze was made of white Plexiglas. Two opposite open and closed quadrants (15 cm walls enclosed two opposing closed quadrants) were placed on circular platform (50 cm diameter, 5 cm width). The platform was elevated 65 cm above ground level. Mice were placed in the center of the closed quadrants and the time spent in each quadrant was recorded for 5 min under fluorescent lights with EthoVision 3.1 (Noldus) software.

RESULTS

Inhibition of miR-9-5p or miR-9-3p using the miRNA sponge

To specifically inhibit the activity of miR-9-3p, I used ‘miRNA sponge’ which is a method for inhibiting endogenous miRNA activity without exerting effects on the complementary strand miRNA (Ebert et al., 2007). It is a transcript consisting of multiple tandem binding sites of miRNA and works as a competitive decoy target for miRNA, which can induce loss-of-function phenotypes and elucidates the functions of endogenous miRNA. I designed miR-9-3p sponge expressing the EGFP genes with 3' UTR containing 6 bulged miR-9-3p binding sites and miR-9-5p sponge expressing the EGFP genes with 3' UTR containing 7 bulged miR-9-5p binding sites. Control sponge expressing the EGFP genes with 3' UTR containing 7 bulged artificial miRNA binding sites which are not target sequences of any known miRNA (Fig. 3 A).

To validate the efficacy of miRNA sponges, I performed luciferase assay in HEK 293T cell. The firefly luciferase expression can be regulated via the miRNA target sequence in the 3' UTR of its mRNA. A single perfect matched target sequence of miR-9-5p or miR-9-5p was inserted in the 3' UTR of mRNA of firefly luciferase, which was named as miR-9-3p sensor or miR-9-5p sensor. Among three genetic loci encoding miR-9-5p/3p in mammals: miR-9-1, miR-9-2 and miR-9-3, I cloned miR-9-2 due to its most abundant expression in mouse brain (Shibata et al., 2011). Overexpression of miR-9-2 reduced the activity of the miR-9-3p sensor, which was reversed by co-transfection of miR-9-3p sponge (n = 5 per group, one-way analysis of variance (ANOVA), $F_{2,12} = 86$, $p < 0.0001$; Fig. 3 B). The activity of miR-9-5p

sensor was also suppressed by miR-9-2 overexpression, which was reversed by co-transfection of miR-9-5p sponge (n = 4 per group, one-way ANOVA, $F_{2,9} = 376.2$, $p < 0.0001$; Fig. 3 C). These results clearly showed that miR-9-3p or miR-9-5p sponges inhibits the activity of miR-9-3p or miR-9-5p.

To express miRNA sponges in neuron, miRNA sponges were subcloned in adeno-associated virus (AAV) vectors. AAV-miRNA sponges were stably expressed in hippocampus under the control of synapsin promoter (Fig. 4 A,B).

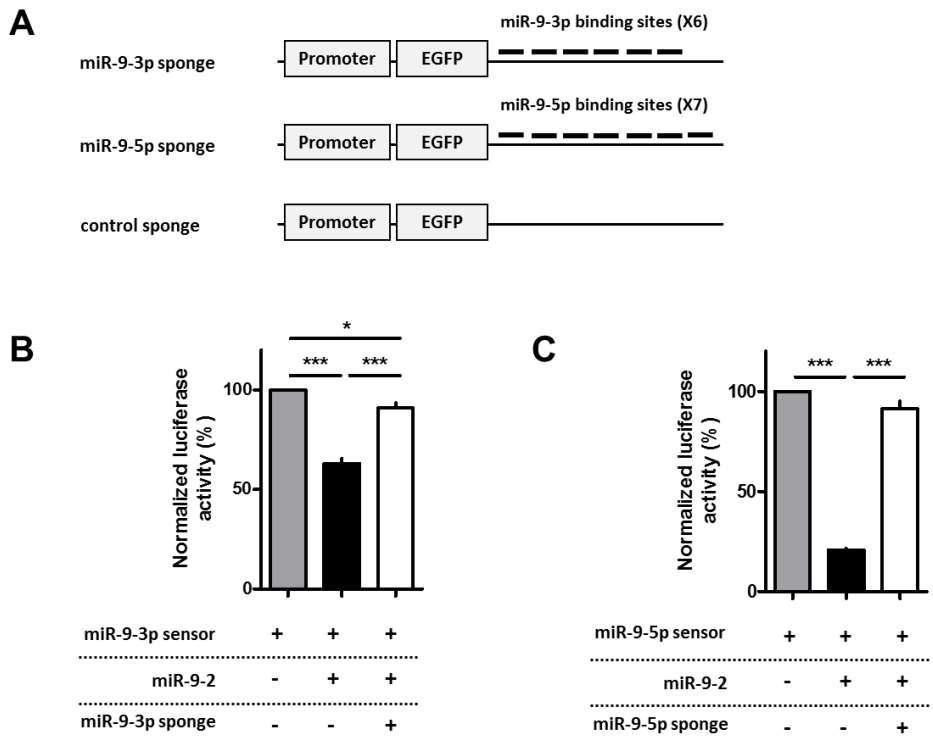

Figure 3. miRNA-sponge systems inhibit the activity of miR-9-5p/3p

(A) Schematic diagrams of miRNA sponge

(B) Luciferase assay shows that miR-9-3p sponge specifically suppresses the activity of miR-9-3p (*$p < 0.05$, ***$p < 0.001$, n = 5 per group, Tukey's multiple comparison test after significant one-way ANOVA).

(C) Luciferase assay shows that miR-9-5p sponge specifically suppresses the activity of miR-9-5p (***$p < 0.001$, n = 4 per group, Tukey's multiple comparison test after significant one-way ANOVA).

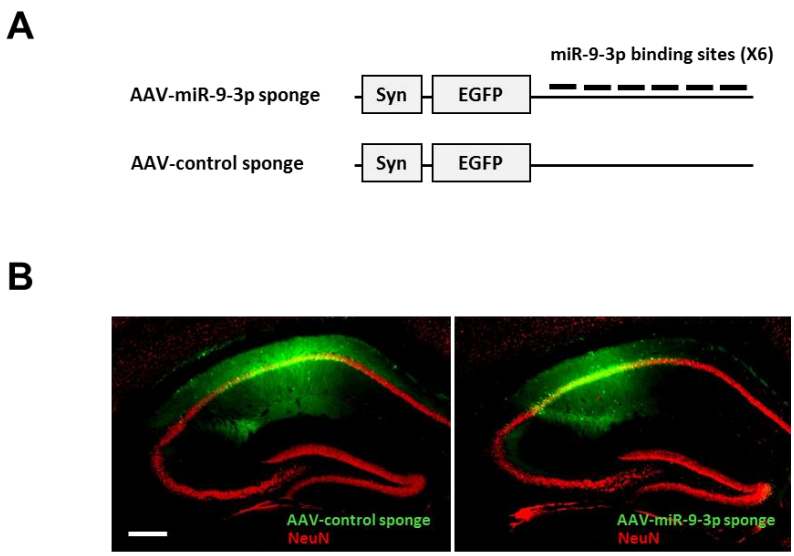

Figure 4. Expression of AAV-miRNA sponge in hippocampus

(A) Schematic diagrams of AAV-miRNA sponge

(B) Representative fluorescence images showing EGFP expression in hippocampus 4 weeks after injection of AAV-miRNA sponge. Scale bar, 300 μm.

Inhibition of miR-9-3p, but not miR-9-5p, impairs LTP

Next, I investigated the role of miR-9-3p in synaptic plasticity at hippocampal SC-CA1 synapses. Whole-cell patch clamp recording was performed after two weeks of expression of AAV-miRNA sponges in CA1 region of hippocampus. miR-9-3p sponge expression significantly reduced the level of theta-burst-induced LTP compared to the control sponge or naïve group (Fig. 5 A). Statistical analysis of the EPSC amplitude of last 5 min of recording showed the significant impairment of LTP in miR-9-3p sponge group (last 5 min of recording, control, n = 6 cells from 3 mice, miR-9-3p, n = 9 cells from 6 mice, naïve, n = 7 cells from 5 mice, one-way ANOVA, $F_{2,19}$ = 9.514, p = 0.0014; Tukey's multiple comparison test, control versus miR-9-3p, miR-9-3p versus naïve, $p < 0.01$; Fig. 5 B)

In addition to LTP, I also examined whether miR-9-3p sponge expression affects long-term depression (LTD) in the CA3-CA1 synapse of the hippocampus (Fig. 6 A). I found that inhibition of miR-9-3p has no significant effect on LTD (last 5 min of recording, control, n = 9 cells from 4 mice, miR-9-3p, n = 7 cells from 3 mice, unpaired two-tailed *t*-test, $t(14) = 0.6813$, $p = 0.5068$; Fig. 6 B)

I examined the role of miR-9-5p in hippocampal LTP, because miR-9-5p has been considered as dominant strand of *miR-9-5p/3p* gene. Unlike miR-9-3p, inhibition of miR-9-5p had no effect on the level of theta-burst LTP (last 5 min of recording, control, n = 12 cells from 7 mice, miR-9-5p, n = 14 cells from 6 mice, unpaired two-tailed *t*-test, $t(24) = 0.8454$, $p = 0.749$; Fig. 7 A,B), demonstrating that only miR-9-3p, but not miR-9-5p is involved in hippocampal LTP.

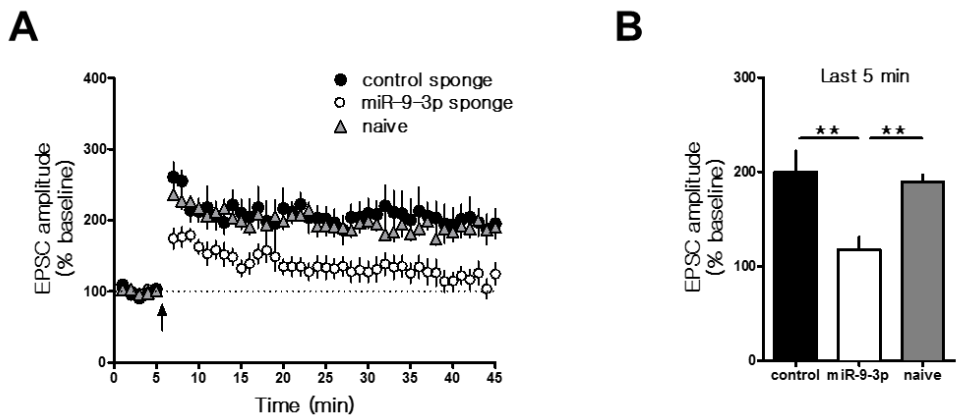

Figure 5. AAV-miR-9-3p sponge-mediated miR-9-3p inhibition blocks hippocampal LTP

(A) Theta-burst LTP recordings was significantly impaired in miR-9-3p sponge expressing neurons.

(B) Summary graph represents the average EPSC amplitudes of the last 5 min recording in naïve, control sponge, and miR-9-3p sponge groups (n = 7, naïve; n = 6, control sponge; n = 9, miR-9-3p sponge, $^{**}p < 0.01$, Tukey's multiple comparison test after one-way ANOVA). Data are mean ± s.e.m.

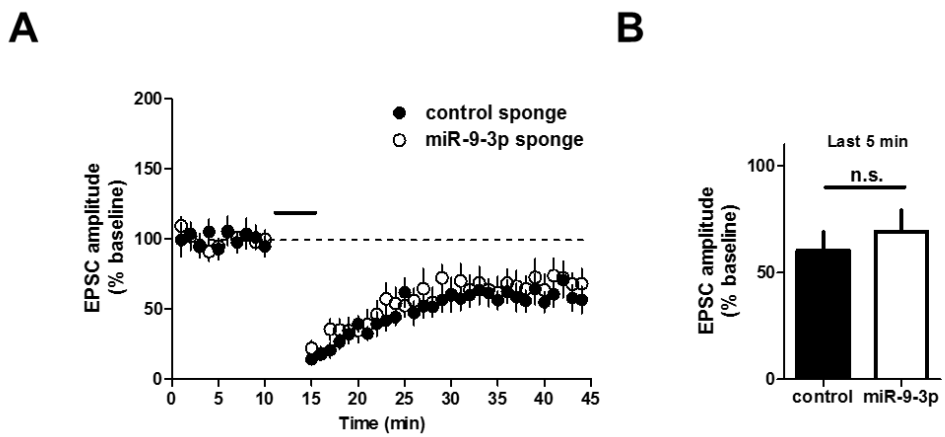

Figure 6. AAV-miR-9-3p sponge-mediated miR-9-3p inhibition has no effect on hippocampal LTD.

(A) Hippocampal LTD was comparable between control and miR-9-5p sponge.

(B) Summary graph represents the average EPSC amplitudes of the last 5 min recording in control and miR-9-3p sponge (control, n = 9 cells from 4 mice, miR-9-3p, n = 7 cells from 3 mice, unpaired two-tailed *t*-test, $t(14) = 0.6813$, $p = 0.5068$). Data are mean ± s.e.m.

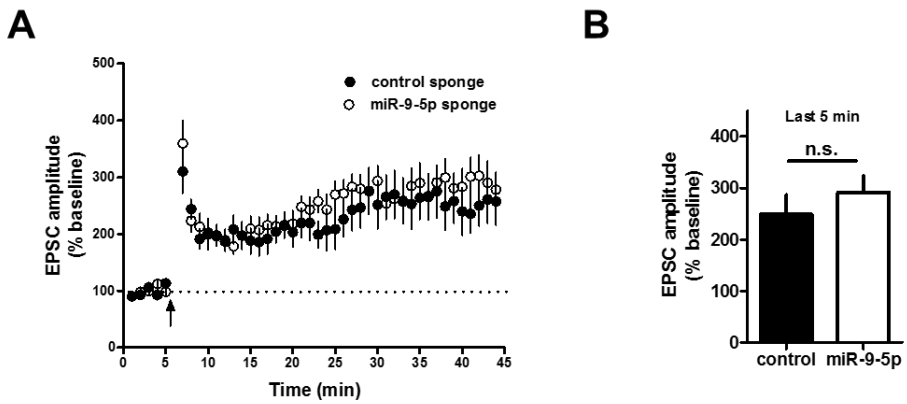

Figure 7. AAV-miR-9-5p sponge-mediated miR-9-5p inhibition has no effect on hippocampal LTP

(A) Theta-burst LTP was comparable between control and miR-9-5p sponge.

(B) Summary graph represents the average EPSC amplitudes of the last 5 min recording in control and miR-9-5p sponge groups (last 5 min of recording, control, n = 12 cells from 7 mice, miR-9-5p, n = 14 cells from 6 mice, unpaired two-tailed *t*-test, $t(24) = 0.8454$, $p = 0.749$). Data are mean ± s.e.m.

Inhibition of miR-9-3p does not affect membrane excitability and basal synaptic transmission

The effect of blocking miR-9-3p activity on intrinsic membrane excitability was examined by measuring action potentials after applying step current pulses in CA1 pyramidal neurons. There were no significant differences in the number of action potentials between groups, suggesting that miR-9-3p sponge expression does not affect the membrane excitability (n = 6 cells from 3 mice per group, two-way ANOVA, $F_{4,45} = 0.11$, $p = 0.9786$; Fig. 8 A).

Next, basal synaptic strength and presynaptic transmission was examined by measuring input-output relationship and paired-pulse facilitation ratio, respectively. Inhibition of miR-9-3p affect neither input-output relationship nor paired-pulse facilitation ratios (input-output relationship, control, n = 8 from 3 mice, miR-9-3p, n = 6 from 3 mice, naïve, n = 7 from 3 mice, two-way ANOVA, $F_{12,126} = 0.07$, $p = 1$; paired-pulse facilitation ratios, n = 6 cells from 3 mice per group, two-way ANOVA, $F_{8,75} = 0.29$, $p = 0.9680$; Fig. 8 B,C).

I also measured spontaneous excitatory and inhibitory postsynaptic currents (sEPSC and sIPSC) and miniature excitatory and inhibitory postsynaptic currents (mEPSC and mIPSC) to test whether blocking miR-9-3p activity affects excitatory or inhibitory synaptic transmission in CA1 pyramidal neurons. However, I found that the frequencies and amplitudes of sEPSC, sIPSC, mEPSC and mIPSC were comparable among neurons expressing miR-9-3p sponge or control sponge, suggesting that inhibition of miR-9-3p activity has no effect on excitatory and inhibitory synaptic transmission (sEPSC, control, n = 6 cells from 3 mice, miR-9-3p, n = 11 cells from 5 mice; mEPSC, control, n = 7 cells from 3 mice, miR-9-3p, n = 9

from 5 mice; sIPSC, control, n = 10 cells from 5 mice, miR-9-3p, n = 9 cells from 4 mice; mIPSC, control, n = 11 cells from 5 mice, miR-9-3p, n = 6 cells from 4 mice; Fig. 9 A-F).

In addition, I examined whether the miR-9-3p sponge treatment affects NMDA receptor function which is known to be critical for LTP induction (Collingridge et al., 1983; Tsien et al., 1996). I found that inhibition of miR-9-3p did not affect input-output relationship of NMDA receptor-mediated EPSC in the presence of CNQX (control, n = 8 cells from 3 mice, miR-9-3p, n = 11 cells from 4 mice; two-way ANOVA, $F_{5,102} = 0.4$, $p = 0.8482$ Fig. 10 A). Furthermore, the I-V plot of miR-9-3p expressing cells was not distinguishable from that of control group (control, n = 11 cells from 3 mice, miR-9-3p, n = 12 cells from 4 mice; two-way ANOVA, $F_{6,147} = 0.11$, $p = 0.995$, Fig. 10 B), suggesting that miR-9-3p does not regulate NMDA receptor function.

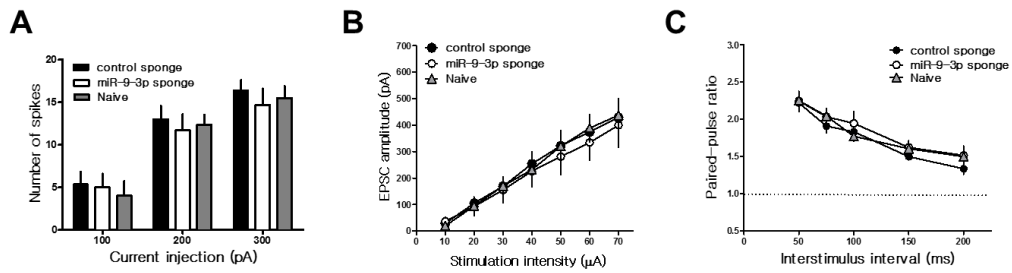

Figure 8. Inhibition of miR-9-3p has no effects on basal synaptic properties

(A) Action potentials were generated by current injection (n = 6 for each group)

(B) Input-output relationship (n = 7, naïve; n = 8, control sponge; n = 6, miR-9-3p sponge)

(C) Paired-pulse ratio at the indicated inter-stimulus intervals (n = 6 for each group)

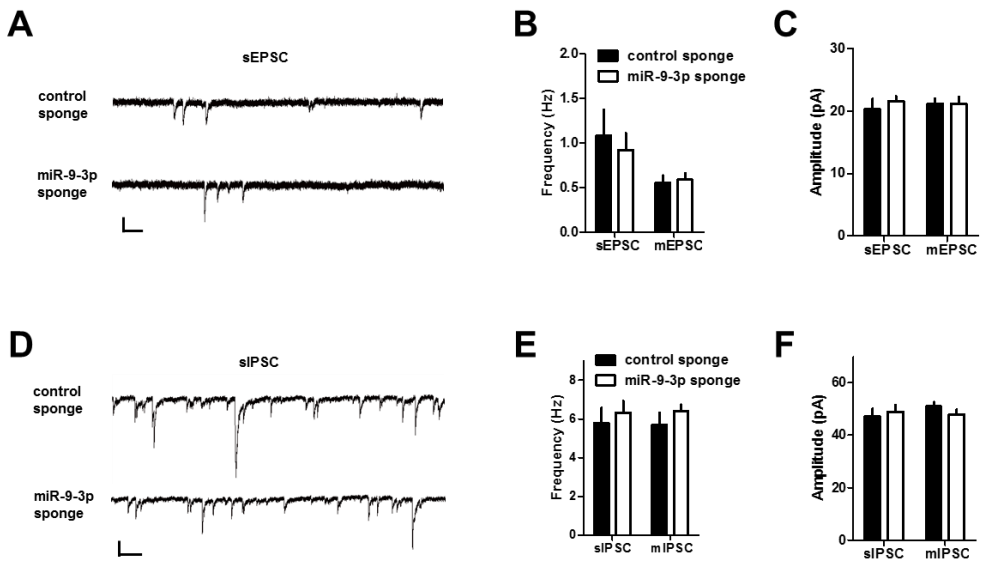
A
sEPSC
control sponge
miR-9-3p sponge
B
control sponge
miR-9-3p sponge
Frequency (Hz)
2.0
1.5
1.0
0.5
0.0
sEPSC
mEPSC
C
Amplitude (pA)
30
20
10
0
sEPSC
mEPSC
D
sIPSC
control sponge
miR-9-3p sponge
E
control sponge
miR-9-3p sponge
Frequency (Hz)
8
6
4
2
0
sIPSC
mIPSC
F
Amplitude (pA)
60
40
20
0
sIPSC
mIPSC

Figure 9. sEPSC, mEPSC, sIPSC and mIPSC were intact in AAV-miR-9-3p sponge expressing group

(A-C) sEPSC and mEPSC from CA1 pyramidal neurons expressing control sponge or miR-9-3p sponge.

(A) Representative sEPSC recording traces. Scale bars, 25 pA and 200 ms. Graphs show sEPSC (n = 6, control sponge; n = 11, miR-9-3p sponge) and mEPSC (n = 7, control sponge; n = 9, miR-9-3p sponge) frequency (B) and amplitude (C).

(D-F) sIPSC and mIPSC from CA1 pyramidal neurons expressing control sponge or miR-9-3p sponge.

(D) Representative sIPSC recording traces. Scale bars, 50 pA and 200 ms. Graphs show sIPSC (n = 10, control sponge; n = 9, miR-9-3p sponge) and mIPSC (n = 11, control sponge; n = 6, miR-9-3p sponge) frequency (E) and amplitude (F). Data are mean ± s.e.m.

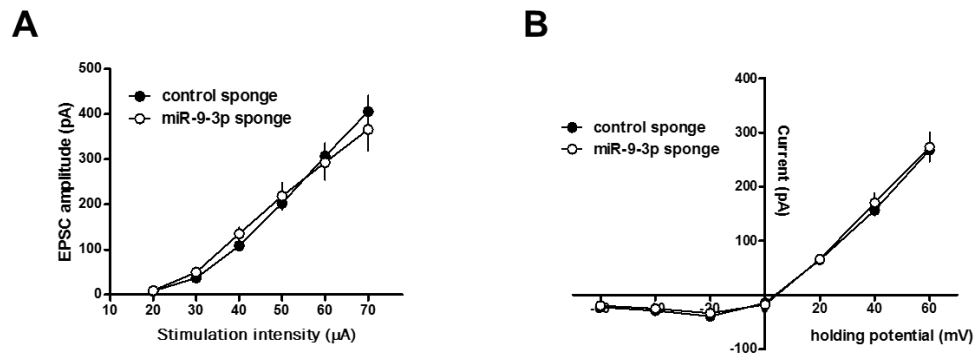

Figure 10. Inhibition of miR-9-3p activity has no effects on NMDAR-mediated synaptic transmission.

(A) Input-output relationship of NMDAR-mediated EPSC (n = 8, control sponge; n = 11, miR-9-3p sponge).

(B) NMDAR-mediated I-V plot (n = 11, control sponge; n = 12, miR-9-3p sponge). Data are mean ± s.e.m.

Inhibition of miR-9-3p activity impairs hippocampus-dependent memory

Next, I examined the behavioral effects of inhibiting miR-9-3p activity via AAV-miRNA sponge infection in the dorsal CA1 region of the adult mouse hippocampus. I first tested mice in the Morris water maze task to examine hippocampus-dependent spatial memory. Control or miR-9-3p sponge-expressing mice showed similar escape latencies during the training sessions (control, n = 9 mice, miR-9-3p, n = 10 mice, repeated-measure two-way ANOVA, the effect of sponge, $F_{1,68} = 0.15$, $p = 0.7062$; Fig. 11 A). However, in the probe test wherein the platform is removed from the pool, miR-9-3p sponge-expressing mice spent significantly less time in the target quadrant than the control sponge-expressing mice (two-way ANOVA, sponge × quadrant, $F_{3,68} = 4.44$, $p = 0.0066$; Bonferroni posttests, target quadrant, control versus miR-9-3p, $p < 0.05$; Fig. 11 B,C), suggesting that blocking miR-9-3p activity impairs spatial memory.

Second, the mice were examined in the object-location recognition task, which exploits the innate nature of mice to explore spatially novel objects and is known to be hippocampus-dependent (Oliveira et al., 2010) (Fig. 12 A). The miR-9-3p sponge-expressing mice failed to recognize the displaced object, while the control sponge-expressing mice showed a significant preference for the displaced object (control, n = 8 mice, one sample paired *t*-test, $t(7) = 4.069$, $p = 0.0048$;miR-9-3p, n = 9 mice, one sample paired *t*-test, $t(8) = 0.9769$, $p = 0.3572$; Fig. 12 B,C).

Finally, I examine the effect of miR-9-3p inhibition on fear memory in trace fear conditioning task, a more demanding hippocampus-dependent behavioral learning paradigm, requiring temporal processing and attention (Huerta et al., 2000; Lim et al., 2014; Zhao et al., 2005). Control and miR-9-3p sponge-expressing mice

displayed similar amounts of freezing levels during the trace fear conditioning training sessions (control, n = 20 mice, miR-9-3p, n = 19 mice, repeated-measures two-way ANOVA, sponge × day, $F_{7,259} = 0.72$, $p = 0.656$; Fig. 13 A). When trace memory was measured 24 h after trace fear conditioning, however, the miR-9-3p sponge group showed significantly less freezing compared to the control sponge group during test sessions (control, n = 20 mice, miR-9-3p, n = 19 mice, repeated-measures two-way ANOVA, sponge × day, $F_{7,259} = 2.02$, $p = 0.0526$; last 4 test sessions (session 4-7), unpaired two-tailed *t*-test, $t(6) = 2.998$, $p = 0.0241$; Fig. 13 B,C). AAV-miR-9-3p-expressing mice showed significantly impaired memory in all of three different hippocampus-dependent tasks.

These results clearly indicate that miR-9-3p has a critical role in hippocampus-dependent memory. Importantly, miR-9-3p sponge expression did not alter either anxiety level or locomotor activity (Fig. 14 A-C).

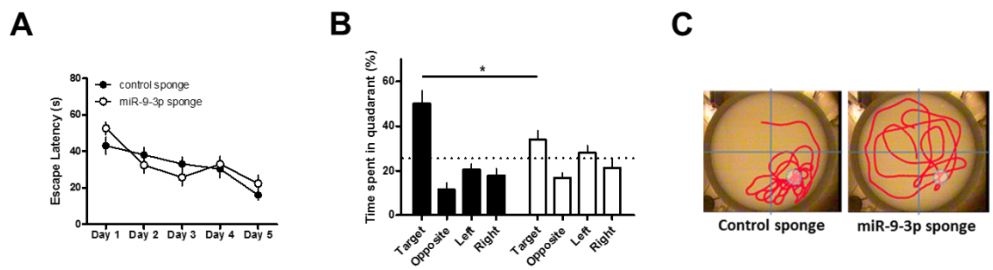

Figure 11. Inhibition of miR-9-3p activity impairs hippocampus-dependent memories: Morris water maze task

(A) Escape latencies to the platform were similar in control and miR-9-3p sponge groups (repeated-measure two-way ANOVA, the effect of sponge, $F_{1,68} = 0.15$, $p = 0.7062$).

(B) Probe test examining time spent in the target quadrant on day 6 showed significant spatial memory deficits in miR-9-3p sponge group (two-way ANOVA, sponge x quadrant, $F_{3,68} = 4.44$, $p = 0.0066$; Bonferroni posttests, $^*p < 0.05$).

(C) Representative images showing the swimming traces of mice during the probe trial. Dashed circle indicates the location of removed platform.

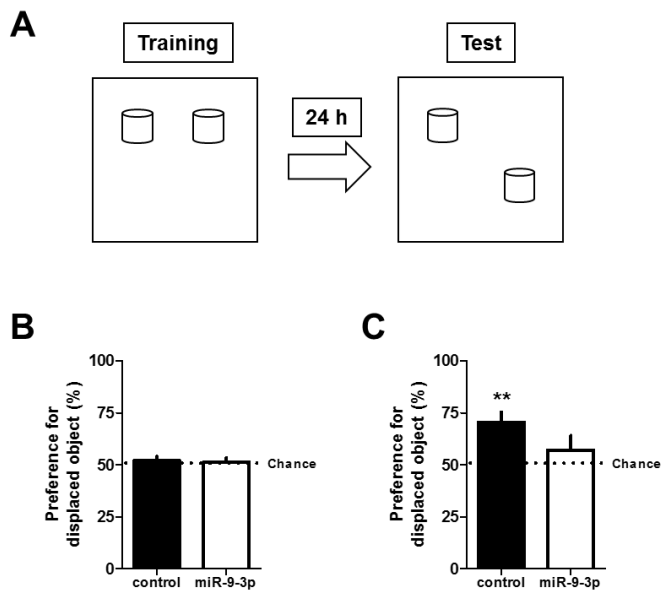

Figure 12. Inhibition of miR-9-3p activity impairs hippocampus-dependent memories: object location memory

(A) Behavior scheme of object location memory

(B) The percentage preference for the objects in the training session.

(C) The percentage preference for the displaced objects in the testing session is reported and the dotted line indicates chance (50%) preference (n = 8, AAV-control sponge; n = 9, AAV-miR-9-3p sponge, one sample paired *t*-test, $^{**}p < 0.01$).

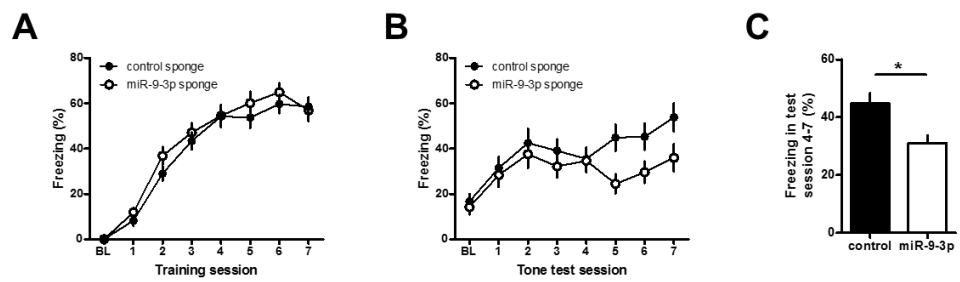

Figure 13. Inhibition of miR-9-3p induces deficits in hippocampus-dependent memory: trace fear conditioning

(A) The average freezing duration during training sessions was similar in control and miR-9-3p sponge group (repeated-measures two-way ANOVA, sponge × day, $F_{7,259} = 0.72$, $p = 0.656$)

(B) Average freezing duration during testing sessions (repeated-measures two-way ANOVA, sponge × day, $F_{7,259} = 2.02$, $p = 0.0526$)

(C) Average freezing duration during testing sessions 4–7 (unpaired two-tailed *t*-test, $*p < 0.05$)

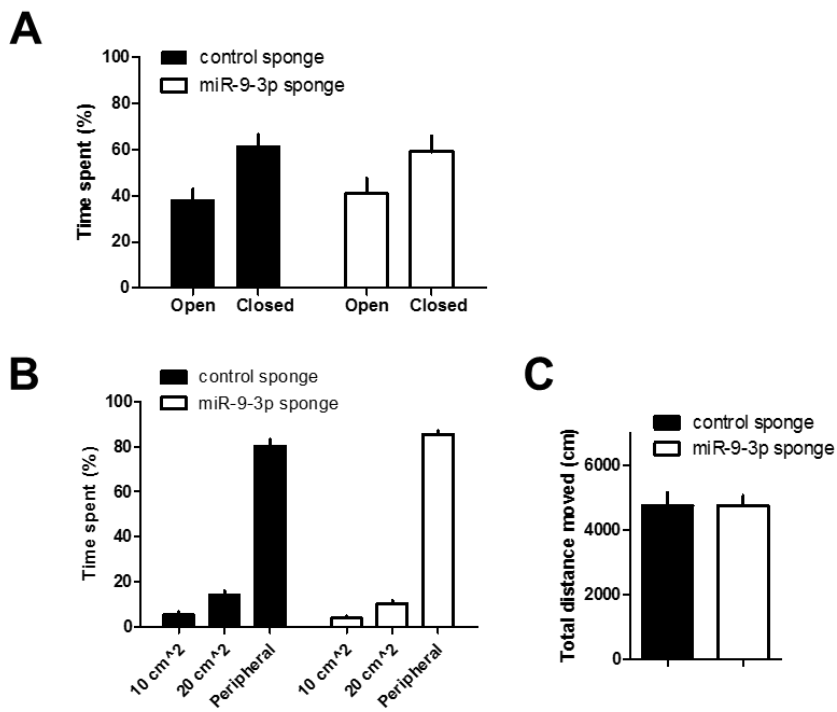

Figure 14. Basal anxiety level and locomotor activity were intact in both AAV-sponge groups

(A) The elevated zero maze test (n = 10, control sponge; n = 11, miR-9-3p sponge)

(B) The open field test (n = 10, control sponge, n = 11, miR-9-3p sponge)

(C) The locomoter activity measured in open field test

DISCUSSION

These results demonstrate that miR-9-3p is critically involved in hippocampal LTP and long-term memory. So far, most of functional studies on miR-9 have highlighted their roles in neuronal development (Dajas-Bailador et al., 2012; Leucht et al., 2008; Otaegi et al., 2011; Shibata et al., 2011). For example, *miR-9-2/miR-9-3* double knockout mice in which both miR-9-5p and miR-9-3p are reduced showed defects in neurogenesis and abnormal telencephalic structures (Shibata et al., 2011). However, miR-9-5p and miR-9-3p are abundantly expressed not only in neural progenitors but also in post-mitotic neurons (Liu et al., 2012; Yuva-Aydemir et al., 2011). Interestingly, miR-9 level was shown to be decreased in the postmortem brains of Huntington's disease patients (Packer et al., 2008) and Alzheimer's disease patients (Cogswell et al., 2008; Hébert et al., 2008), suggesting that miR-9 might be involved in normal brain functions in adult. Recently, Giusti and colleagues showed that inhibition of miR-9-5p using sponge technique impairs dendritic growth as well as excitatory synaptic transmission (Giusti et al., 2014). Interestingly, miR-9-3p sponge had no effect on dendritic growth of cultured neurons (Giusti et al., 2014), which is consistent with my finding that miR-9-3p sponge did not affect basal synaptic transmission.

Many previous studies, especially initial studies, examine the role of miR-9-5p/3p through overexpressing or deleting both miR-9-5p/3p (Bonev et al., 2011; Leucht et al., 2008; Shibata et al., 2011; Zhao et al., 2009), which may lead non-specific results. Because a single mature miRNA family regulates hundreds of target genes, there must be huge discrepancy in gene expression between manipulation of

a single mature miRNA and that of two mature miRNAs. Several methods are known to specifically inhibit a single miRNA family. First, 2'-*O*-methylated antisense oligonucleotide inhibits miRNA in sequence specific manner. 2'-*O*-methyl modification has advantages in less degradation of oligonucleotides and stable hybridization to single-stranded RNA (Meister et al., 2004; Schratt et al., 2006). Second, a locked nucleic acid (LNA) antisense oligonucleotide has high affinity to miRNAs and inhibits them efficiently. The ribose ring is connected by an extra methylene bridge between the 2'-O- and 4'-C-atom, which increases binding efficiency to complementary nucleotide (Vester and Wengel, 2004). Third, microRNA sponge inhibits specific miRNAs as a competitive inhibitor. It is a transcript which consists of multiple, tandem binding sites of target miRNAs and can be stably transcribed from transgenes under strong promoters (Ebert et al., 2007). Compared to relatively short term effect of 2'-*O*-methylated antisense oligonucleotide and LNA antisense oligonucleotide, miRNA sponge has an advantage of long-lasting miRNA inhibition. It can assay long-term effect of miRNA inhibition in cell lines and even transgenic model organisms such as fly, worm and mouse (Giusti et al., 2014; Loya et al., 2009). Therefore, in this study, I chose microRNA sponge to reveal physiological phenotype of miR-9-5p/3p loss-of-function.

CHAPTER 3.

Molecular mechanisms of miR-9-3p

INTRODUCTION

In the first report of miRNA, it was shown that the sequence of miRNA, *lin-4*, is complementary to 3' UTR of target mRNA, *lin-14*. In addition, 3' UTR of lin-14 was necessary and sufficient to lin-4 mediated suppression (Lee et al., 1993; Wightman et al., 1993). Therefore, it was clear that the base-pairing of miRNA-mRNA must be critical. Then, some questions could arise from these results. How does miRNA recognize its target? Should the sequence of mRNA be perfectly matched to all 22 nucleotide-long miRNA sequence? How many sequence of mRNA should be matched with sequence of miRNA to accomplish miRNA-mediated suppression? Subsequent studies combined with computational analyses have answered these questions (Bartel, 2009). Most importantly, 5' region of miRNA, especially position 2-7, is critical to identify target. The nucleotide sequence of 2-7 position of miRNA is called as 'miRNA seed'. The perfect Watson-Crick base-pairing of seed is the most stringent requirement for target identification of miRNA.

There are five types of miRNA target site. First, when the target site only satisfy seed sequence of miRNA, this site type refers to as '6mer site'. Second, additional A residue across position 1 of the miRNA increases efficacy of site binding, which is called '7mer-A1 site'. Third, additional base-pairing of position 8 of miRNA increase efficacy of site binding, which is called '7mer-m8 site'. Fourth, if target sequence satisfies all of previous conditions, it is referred to as '8mer site'. The relative mean efficacies of these miRNA sites are different (8mer >> 7mer-m8 > 7mer A1 >> 6mer). Finally, in very rare case, mismatches or bulged nucleotides exist in the seed matching region, which is called 'atypical sites'. This sites occurs

~1% of miRNA target site.

In addition to type of miRNA target site, the context of target site also influence the efficacy of miRNA target sites. First, a single sites in a single 3' UTR can suppress gene expression, but multiple sites produce more effective suppression (Doench and Sharp, 2004). Second, close target sites tent to operate synergistically (Grimson et al., 2007). The distance should be within 40 nucleotide, but no closer than 8 nucleotide. Third, target sites should be located at least 15 nucleotide from the stop codon. Fourth, the target sites located in the center of long 3' UTR tend to be less efficient. Fifth, AU-rich elements near the target sites increase the efficacy.

TargetScan algorithm is the one of the most widely used miRNA target prediction tools (Grimson et al., 2007; Lewis et al., 2005; Lewis et al., 2003). It predicts targets and ranks ordering of the targets considering previously mentioned features. When its prediction accuracy was compared to other target prediction algorithms including miRBase Target (Griffiths-Jones et al., 2008), miRanda (John et al., 2004), PicTar (Krek et al., 2005), and PITA (Kertesz et al., 2007), TargetScan showed most reliable prediction (Baek et al., 2008). The accuracy of prediction algorithms was examined by comparing with actual proteomics by quantitative mass spectrometry in *miR-233* deficient mouse neutrophils. TargetScan algorithm predicts an average of 300 targets per miRNA family which has same seed sequence (Friedman et al., 2009).

In this chapter, I investigate the molecular mechanism of miR-9-3p. TargetScan algorithm was used to find tentative targets of miR-9-3p. Functional annotation of predicted genes via Gene Ontology narrow downed target genes which are only involved with LTP and memory. Finally, I examined whether the translation

of target genes was regulated by miR-9-3p using luciferase reporter assay and western blotting.

EXPERIMENTAL PROCEDURES

Animals

Male C57BL/6N mice were used for all experiments. 8-week-old mice were purchased from Orient Bio. Inc. Korea. Mice were keep on a 12/12 h light/dark cycle in standard laboratory cages with access to food and water ad libitum. Mice were cared for in accordance with the regulation and guidelines of Institutional Animal Care and Use Committees (IACUC) of Seoul National University.

Target gene prediction of brain-enriched miRNAs

Brain-enriched miRNAs were selected based on a previous study which analyzed mature miRNA profiles from glutamatergic neurons (He et al., 2012). To predict the target genes of miR-9-3p in the mouse hippocampus, a series of bioinformatics analyses were performed. Among the putative candidates genes predicted by TargetScan version 6.2, the top 25% genes based on the context+ score (Garcia et al., 2011) were selected and genes which have only 6mer sites in their 3' UTRs were removed. To identify genes with highly conserved target sequences, target sequences including ≥ 1 nucleotide with a <0.5 PhyloP conservation score were removed (phyloP60way, mm10, UCSC genome browser-http://genome.ucsc.edu (Kent et al., 2002)). After further removing genes whose mRNA expression in the mouse hippocampus did not fall in the top 10,000 highly expressed genes, the target genes of brain-enriched miRNAs were finally obtained. Next, I performed a gene ontology and network analysis by using the Ingenuity Pathway Analysis (QIAGEN, CA) to identify the number of genes whose functional annotations are related with

excitatory synapses, LTP and learning and memory (see Figure 15). Among target genes of miR-9-3p, I identified genes whose loss or gain of function induce any changes in LTP by searching previously published literature and >1 PhyloP conservation scores. Accordingly, 7 final target genes of miR-9-3p were obtained (see Table 2).

Luciferase assay

To validate the miR-9-3p target genes, I cloned the 3' UTR from each of the putative target genes downstream of the firefly luciferase coding region in modified pGL3 luciferase reporter vectors (pGL3-UC). Primers used for cloning are listed in Table S3. The vector was a generous gift of Dr. Narry V. Kim (Seoul National University). The mutation of target sequence was produced by mutagenesis kit (Enzynomics). HEK293T cells were transfected in 12-well plates with 300 ng of firefly luciferase reporter, 200 ng of pcDNA3-renila luciferase and 20 nM of the synthetic miRNA duplexes or negative control duplexes (Bioneer) using Lipofectamine 2000 (Invitrogen). Dual-Glo luciferase assays (Promega) were performed 24 h after transfection according to the manufacturer's instructions. To generate the miR-9-5p/3p expression construct, the miR-9-3p gene was amplified from the genomic locus of mouse miR-9-3p and cloned into a pcDNA3 vector (Invitrogen).

Western blots

The expression of the AAV-miR-9-3p or AAV-control sponge was confirmed by fluorescence microscopy and only the CA1 regions expressing EGFP were collected and frozen in liquid nitrogen for western blot analysis. Samples were homogenized

using the TissueLyser LT (Qaigen) with homogenization buffer (320 mM sucrose, 10 mM HEPES, pH 7.4) containing protease inhibitor cocktail (Roche). The homogenized suspension was centrifuged at 1,000 g for 10 min at 4℃. The supernatant was centrifuged at 12,000 g for 20 min at 4℃ to obtain the pellet (the crude synaptosomal membrane). The pellet was resuspended in radio-immuno-precipitation assay buffer (20 mM HEPES, 0.15 mM NaCl, 1% Triton X-100, 1% sodium deoxycholate, 1% sodium dodecyl sulfate, 1 mM dithiothreitol, pH 7.5) containing protease inhibitor cocktail, followed by rotation (1 h, 4℃) and centrifugation (10,000 g 15 min, 4℃). The supernatant was collected and its protein level was measured by a BCA protein assay (Pierce). Equal amounts of protein were subjected to SDS-PAGE and western blots with the following antibodies: Dmd (sc-73592, Santa Cruz Biotech., 1:200), SAP97 (75-030, Neuromab, 1:1,000) and pan-cadherin (sc-59876, Santa Cruz Biotech., 1:20,000).

RESULTS

Bioinformatic analyses

To identify molecular target of miR-9-3p, I performed a series of bioinformatics analyses (Fig. 15). I also selected 14 excitatory neuron-enriched miRNAs including miR-9-3p and performed same bioinformatics analysis to get more information. The 14 excitatory neuron-enriched miRNAs was selected based on previous cell-type specific miRNA profiling study (He et al., 2012). I used TargetScan algorithm for prediction of tentative target gene. Among the predicted targets, mRNAs harboring evolutionarily conserved miR-9-3p target sequence and expressed in the hippocampus were selected. Next, I accessed the Ingenuity Pathway Analysis (https://analysis.ingenuity.com) to identify the genes whose functional annotations are related to LTP and memory. The number of target genes resulting from each analysis was represented in Table 1. I found that miR-9-3p had 20 putative target genes related in LTP and memory. Then, I performed extensive literature search and selected 7 final candidate target genes whose loss or gain of function induce any change in LTP (Table 2).

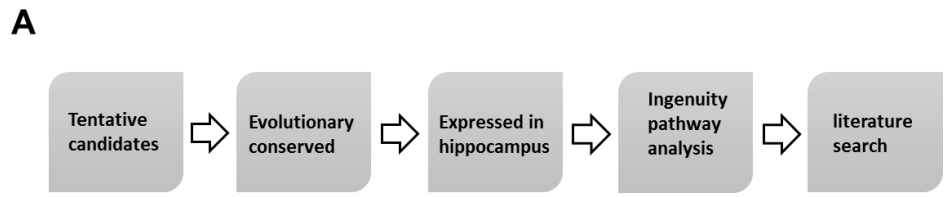

Figure 15. Flow chart of bioinformatic analyses

TargetScan algorithm predicted tentative target genes of miR-9-3p. Further analyses were performed based on evolutionary conservation of miR-9-3p target sequence and reliable expression in hippocampus. Final candidate target genes were identified via Ingenuity Pathway Analysis and literature search.

Bioinformatics						Gene Ontology
miRNAs	Putative candidates	Top25%	Excluding 6mer	Evolutionary Conserved	Expressed in hippocampus	LTP and L&M related genes
miR-9-5p	4993	1294	1194	351	245	20
miR-9-3p	4045	1040	998	224	172	20
miR-124-3p	6294	1573	1382	478	345	31
miR-128-3p	6064	1568	1507	313	241	26
miR-29a-3p	3968	1037	963	262	174	14
miR-22-3p	4857	1230	1118	128	102	11
let-7a-5p	3145	815	782	244	149	8
miR-376a-3p	475	122	121	9	6	1
miR-26a-5p	4543	1120	1077	294	228	20
miR-369-3p	4022	1053	1008	228	180	21
miR-103-3p	5546	1398	1147	216	168	12
miR-125b-5p	4491	1151	1083	179	136	8
miR-16-5p	5738	1474	1360	300	228	21
miR-138-5p	3873	969	940	124	96	12

Table 1. The number of target genes of brain-enriched miRNAs

The number of target genes was counted using a series of bioinformatics and GO analysis.

Gene Symbol	Refseq ID	Description	Type*	Context+ Score	Min phyloP†	LTP change by gene manipulation		References
						Gain of function	Loss of function	
Dmd	NM_007868	dystrophin, muscular dystrophy	7merm8, 7merm8	-0.2611	1.42, 1.45	ND	↑	(Vaillend et al., 1999; Vaillend et al., 2004)
Dlg1 (SAP97)	NM_001252435	discs, large homolog 1	7merm8	-0.19174	1.95	↓	Not affected	(Nakagawa et al., 2004a; Howard et al., 2010; Li et al., 2011)
Myh10	NM_175260	myosin, heavy polypeptide 10, non-muscle	8mer	-0.181	3.25	ND	↓	(Rex et al., 2010)
Cacng2 (Stargazin)	NM_007583	calcium channel, voltage-dependent, gamma subunit 2	8mer	-0.18095	3.36	Serine 9 phosphorylation-dependent bidirectional synaptic plasticity		(Tomita et al., 2005)
Lrrtm1	NM_028880	leucine rich repeat transmembrane neuronal 1	7merm8	-0.17026	1.53	ND	↓	(Soler-Llavina et al., 2013)
Cdh2	NM_007664	cadherin 2	7merA1, 7merA1	-0.16819	1.20, 4.29	ND	↓	(Tang et al., 1998; Bozdagi et al., 2000)
Ppp3r1	NM_024459	protein phosphatase 3, regulatory subunit B, alpha isoform (calcineurin B, type I)	7merA1	-0.13017	2.84	ND	Threshold shift	(Zeng et al., 2001)

Table 2. List of final candidate target genes of miR-9-3p

*Type of miRNA target sequences depending on seed-matching (Bartel, 2009)

†Minimum PhyloP conservation score of target sequences

ND: not determined

miR-9-3p suppresses the expression of LTP-related genes

I validated that miR-9-3p suppresses the expression of luciferase reporter constructs containing the 3' UTRs of candidate target genes in *in vitro* luciferase assays (n = 4 - 6 for each group, two-way ANOVA, miR-9-3p × mutation; *Dmd*, $F_{1,20} = 5.91$, $p = 0.0245$; *SAP97*, $F_{1,20} = 9.59$, $p = 0.0057$; *Stg*, $F_{1,20} = 14.97$, $p = 0.001$; *Myh10*, $F_{1,20} = 31.39$, $p < 0.0001$; *Cdh2*, $F_{1,12} = 8.95$, $p = 0.0112$; *Lrrtm1*, $F_{1,12} = 27.5$, $p = 0.0002$; *Ppp3r1*, $F_{1,12} = 7.06$, $p = 0.0209$; Bonferroni posttests, 3' UTR (wt) + control siRNA versus 3' UTR (wt) + miR-9-3p, $^{**}p < 0.01$, $^{***}p < 0.001$; Fig. 16 A,B). For 6 of the 7 candidate target genes, miR-9-3p suppressed the translation of luciferase reporter. The mutation of target sequence within 3' UTRs diminished the effect of miR-9-3p, indicating the specific binding of miR-9-3p to the 3' UTR of candidate target genes.

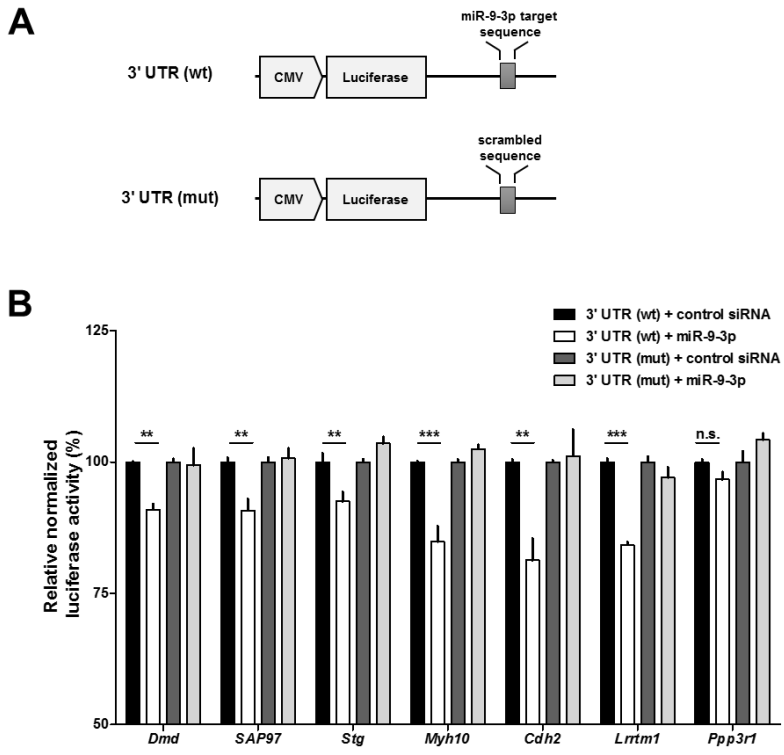
A
miR-9-3p target sequence
3' UTR (wt)
CMV
Luciferase
scrambled sequence
3' UTR (mut)
CMV
Luciferase
B
3' UTR (wt) + control siRNA
3' UTR (wt) + miR-9-3p
3' UTR (mut) + control siRNA
3' UTR (mut) + miR-9-3p
Relative normalized luciferase activity (%)
125
100
75
50
**
**
**
***
**
***
n.s.
Dmd
SAP97
Stg
Myh10
Cdh2
Lrrtm1
Ppp3r1

Figure 16. miR-9-3p regulates the expression of LTP-related genes

(A) Schematic diagrams of the reporter constructs used for the luciferase assays.

(B) miR-9-3p suppresses the expression of the luciferase reporters containing the 3' UTRs of selected LTP-related genes (n = 4 ~ 6 for each group, two-way ANOVA, miR-9-3p × mutation; *Dmd*, $F_{1,20} = 5.91$, $p = 0.0245$; *SAP97*, $F_{1,20} = 9.59$, $p = 0.0057$; *Stg*, $F_{1,20} = 14.97$, $p = 0.001$; *Myh10*, $F_{1,20} = 31.39$, $p < 0.0001$; *Cdh2*, $F_{1,12} = 8.95$, $p = 0.0112$; *Lrrtm1*, $F_{1,12} = 27.5$, $p = 0.0002$; *Ppp3r1*, $F_{1,12} = 7.06$, $p = 0.0209$; Bonferroni posttests, 3' UTR (wt) + control siRNA versus 3' UTR (wt) + miR-9-3p, $^{**}p < 0.01$, $^{***}p < 0.001$).

Dmd and *SAP97* are novel molecular targets of miR-9-3p

Based on the role of miRNAs in translational repression, inhibition of miR-9-3p via miRNA sponge should increase the expression of target gene. The increased expression level of target gene may impaired hippocampal LTP. Therefore, I hypothesized that the genuine targets of miR-9-3p were negatively correlated with LTP. Among 7 candidate target genes, *Dmd* (also known as *dystrophin*) and *SAP97*(also known as *Dlg1*) showed negative correlation with LTP: *Dmd* deficient mice showed enhanced LTP (Vaillend et al., 2004a) and *SAP97* overexpression impaired LTP (Li et al., 2011; Nakagawa et al., 2004a). Therefore, I focused on *Dmd* and *SAP97* as molecular targets of miR-9-3p.

Bioinformatic analysis identified that both *Dmd* and *SAP97* 3' UTRs contain highly conserved miR-9-3p target sequence (Fig. 17 A and Fig. 18 A). To validate whether *Dmd* and *SAP97* are genuine targets of miR-9-3p *in vivo*, I expressed control and miR-9-3p sponge in the dorsal CA1 region for 4 weeks and performed western blots with only the CA1 regions expressing EGFP. I confirmed that the protein levels of Dmd and SAP97 in the hippocampus were significantly increased by inhibiting miR-9-3p (Dmd, control, 100.0 ± 13.97%, n = 7 hippocampi, miR-9-3p, 156.2 ± 14.87%, n = 8 hippocampi, unpaired two-tailed *t*-test, $t(13) = 2.724$, $p = 0.0173$; SAP97, control, 100.0 ± 1.188%, n = 5 hippocampi, miR-9-3p, 125.2 ± 7.792%, n = 4 hippocampi, unpaired two-tailed *t*-test, $t(7) = 3.606$, $p = 0.0087$; Fig. 17 B,C and Fig. 18 B,C). Taken together, these results suggest that miR-9-3p regulates LTP and memory by maintaining optimal expression levels of LTP-related genes such as *Dmd* and *SAP97*.

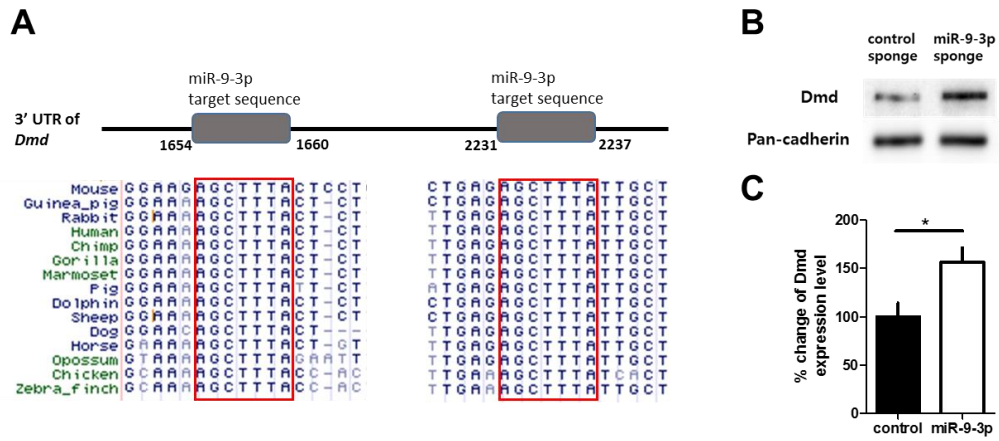

Figure 17. *Dmd* is a novel target of miR-9-3p

(A) Bioinformatic analyses identified highly conserved miR-9-3p target sequences within *Dmd* 3' UTR.

(B) Representative western blot images of Dmd

(C) Dmd protein level was significantly increased in the hippocampi overexpressing miR-9-3p sponge (n = 7, AAV-control sponge; n = 8, AAV-miR-9-3p sponge, unpaired two-tailed *t*-test, $*p < 0.05$).

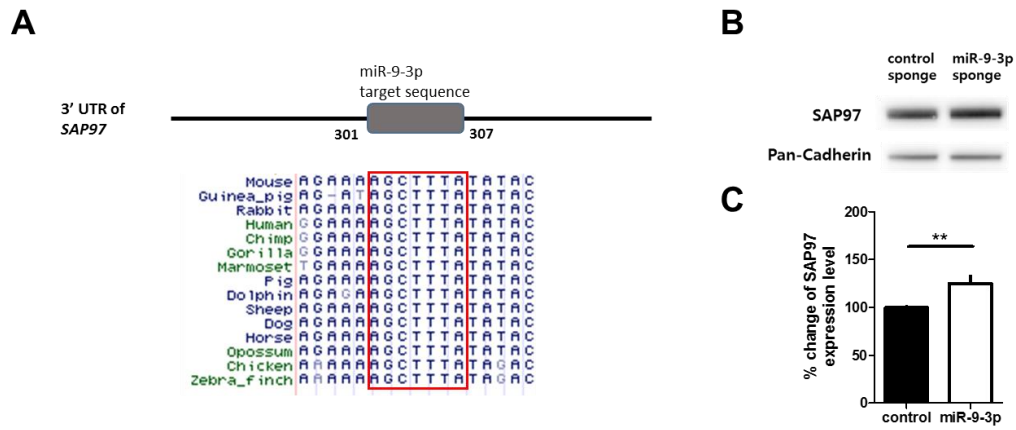

Figure 18. SAP97 is another novel target of miR-9-3p

(A) Bioinformatic analyses identified highly conserved miR-9-3p target sequences within *SAP97* 3' UTR.

(B) Representative western blot images of SAP97

(C) SAP97 protein level was significantly increased in hippocampi overexpressing the miR-9-3p sponge (n = 5, AAV-control sponge; n = 4, AAV-miR-9-3p sponge, unpaired two-tailed *t*-test, $^{**}p < 0.01$). Data are mean ± s.e.m.

DISCUSSION

Dystrophin is large 427 kDa cytoskeletal protein responsible for chromosome X-linked Duchenne muscular dystrophy (DMD) that affects approximately 1 in 3300 male births (Emery, 1991; Hoffman et al., 1987). Absence or mutation in *Dmd* gene causes membrane instability in muscles, thereby inducing Duchenne muscular dystrophy (DMD) whose symptoms are severe muscle degradation and progressive muscular weakness. Besides the features of DMD in skeletal muscle, DMD patients also show non-progressive cognitive impairments, which implies critical roles of *Dmd* in brain. The animal model of DMD, *mdx* mouse, showed the impairment of memory consolidation in certain behavior tasks (Muntoni et al., 1991; Sicinski et al., 1989; Vaillend et al., 2004a; Vaillend et al., 1995), supporting the importance of *Dmd* in cognitive function. Interestingly, slice filed recording in *mdx* mice showed the increase of synaptic strength after intensive stimulus (Vaillend et al., 2004b; Vaillend et al., 1999). Here, I observed that the increase of dystrophin via AAV-miR-9-3p sponge reduced the induction level of LTP. Together, it can be interpreted that negative correlation exists between the expression level of dystrophin and the induction level of LTP. Although it remains unknown whether miR-9-3p level is altered in DMD patients, this finding showing down-regulation of *Dmd* by miR-9-3p may provide a new insight into developing treatments of cognitive impairment in DMD patients.

I hypothesize that mRNA of dystrophin is localized to synapse while its translation is inhibited by miR-9-3p. Two features of dystrophin support my hypothesis. First, the size of dystrophin gene is ~2.5 Mb encoding a 14 kb mRNA transcript which takes 16 h to transcribe (Tennyson et al., 1995). In the aspect of

optimizing energy cost, post-transcriptional regulation of dystrophin would be more efficient rather than *de novo* transcription of dystrophin gene. Second, the expression of dystrophin is restricted to PSD (Kim et al., 1992; Lidov et al., 1990). This localized protein distribution supports local protein synthesis may play a crucial role for its regulation of expression. Moreover, there are other evidences supporting the post-transcriptional regulation of dystrophin via miRNAs. The expressions of miR-31 and miR-206 were up-regulated in the muscle of *mdx* mouse. Especially, miR-31 directly regulates mRNA of dystrophin in myoblast (Cacchiarelli et al., 2011).

SAP97 is the only member of PSD-95-like membrane associated guanylate kinases (PSD-MAGUKs) which directly binds to C-terminal of GluA1 and is involved in AMPA receptor (AMPAR) trafficking (Cai et al., 2002; Leonard et al., 1998). For example, Nash and colleagues showed that SAP97-myosin VI complex plays critical role in trafficking of AMPARs to synapses (Nash et al., 2010). However, its role in excitatory synaptic transmission and AMPAR trafficking is controversial. Some researchers have reported that overexpressing SAP97 enhances mEPSC frequency or evoked EPSC amplitude (Nakagawa et al., 2004b; Rumbaugh et al., 2003) while others have shown that overexpressing SAP97 has no effect (Schlüter et al., 2006; Schnell et al., 2002). The effects of SAP97 overexpression on synaptic transmission seem to be influenced by many factors such as isoforms of SAP97 (Schlüter et al., 2006; Waites et al., 2009), compensation with other PSD-MAGUKs (Howard et al., 2010; Schlüter et al., 2006) or matureness of synapse (Howard et al., 2010). In the present study, SAP97 was increased by miR-9-3p inhibition but I could not detect any changes in excitatory synaptic transmission (Fig. 9 A-C and Fig. 18 B,C). This result is consistent with a previous result showing no effect of SAP97

overexpression on synaptic transmission in mature neurons (Howard et al., 2010). On the other hand, the effect of overexpressing SAP97 on LTP is rather clear. When pairing-LTP or chemical LTP stimulus was given, SAP97 overexpressed neurons showed LTP deficits (Li et al., 2011; Nakagawa et al., 2004b), which is consistent with my LTP results.

Furthermore, I showed that miR-9-3p inhibition did not affect NMDAR function, suggesting that miR-9-3p is involved in LTP induction highly likely through regulating AMPAR trafficking. Depending on the stimulation paradigms, LTP can be divided into two forms: PKA and protein synthesis-dependent and PKA and protein synthesis-independent form (Park et al., 2016). The induction of PKA-sensitive LTP requires multiple episodes of stimuli with proper inter-episode intervals (Kim et al., 2010; Park et al., 2016; Park et al., 2014; Woo et al., 2003). In my experiments, LTP was induced by applying theta burst stimulation with relatively short intervals, which may not be sensitive to protein synthesis and PKA inhibitors. Considering that miRNAs regulate the protein translation, it would be of interest to examine whether miR-9-3p is also involved in protein synthesis-dependent form of LTP.

CHAPTER 4. CONCLUSION

CONCLUSION

In the present study, I provide the first evidence for the adult function of miR-9-3p in mammalian adult brain combining electrophysiological, behavioral, computational and molecular approaches.

In chapter II, I investigated the function of miR-9-3p in hippocampal synaptic plasticity and memory. I established miR-sponge systems to inhibit the activity of miR-9-5p or -3p and delivered AAV-miR-sponges in CA1 region of hippocampus. Using whole cell patch recording, the effect of miR-9-5p or 3p was examined *in vivo* and confirmed that miR-9-3p, but not miR-9-5p, is critical for hippocampal LTP. Meanwhile, the activity of miR-9-3p has no effect on hippocampal LTD, NMDAR function and basal synaptic transmission. Then, I showed that inhibition of miR-9-3p *in vivo* impairs hippocampus-dependent memory in three different behavioral tasks: Morris water maze, object location memory and trace fear conditioning. These results clearly showed the functional importance of miR-9-3p in hippocampal synaptic plasticity and memory.

In chapter III, I found a novel molecular mechanism of miR-9-3p. I predicted the tentative target genes of miR-9-3p via a series of bioinformatics analyses. Among predicted target genes, 7 LTP-related genes were selected by comprehensive literature search. Then, I showed that the 3' UTRs of these LTP-related genes were suppressed by mR-9-3p. Based on the role of miRNAs in translational repression, I focused on genes which are negatively related with LTP, *Dmd* and *SAP97*, and found out the protein expression of Dmd and SAP97 are suppressed by miR-9-3p. These results demonstrate that the effects of miR-9-3p on

hippocampal LTP and memory are mediated by regulating the expression of Dmd and SAP97, which suggests a novel molecular mechanism of miR-9-3p.

Several questions were remained for future studies. First, most of pre-miRNAs produce only one mature miRNA via strand selection, but pre-miR-9 produce two mature miRNAs which both are highly expressed in brain, evolutionary conserved and ancient. It would be interesting to investigate the evolutionary driving force for miR-9-5p/3p evolution. Second, in this study, I only focused on the role of miR-9-3p on hippocampus. However, considering the number of target genes of miR-9-3p, miR-9-3p might have various functions in other brain regions or circumstances. One possibility is a neuroprotective role in neurodegenerative disease. Since the expression level of miR-9-3p was decreased in both Huntington's disease and Alzheimer's disease patients, it might be worth to investigate the role of miR-9-3p in these diseases.

REFERENCES

Atkins, C.M., Selcher, J.C., Petraitis, J.J., Trzaskos, J.M., and Sweatt, J.D. (1998). The MAPK cascade is required for mammalian associative learning. Nature neuroscience *1*, 602-609.

Baek, D., Villén, J., Shin, C., Camargo, F.D., Gygi, S.P., and Bartel, D.P. (2008). The impact of microRNAs on protein output. Nature *455*, 64-71.

Bartel, D.P. (2004). MicroRNAs: genomics, biogenesis, mechanism, and function. cell *116*, 281-297.

Bartel, D.P. (2009). MicroRNAs: target recognition and regulatory functions. Cell *136*, 215-233.

Berezikov, E., Cuppen, E., and Plasterk, R.H. (2006). Approaches to microRNA discovery. Nature genetics *38*, S2-S7.

Bliss, T.V., and Collingridge, G.L. (1993). A synaptic model of memory: long-term potentiation in the hippocampus. Nature *361*, 31-39.

Bliss, T.V., and Lømo, T. (1973). Long-lasting potentiation of synaptic transmission in the dentate area of the anaesthetized rabbit following stimulation of the perforant path. The Journal of physiology *232*, 331-356.

Bohnsack, M.T., Czaplinski, K., and GÖ RLICH, D. (2004). Exportin 5 is a RanGTP-dependent dsRNA-binding protein that mediates nuclear export of pre-miRNAs. Rna *10*, 185-191.

Bonev, B., Pisco, A., and Papalopulu, N. (2011). MicroRNA-9 reveals regional diversity of neural progenitors along the anterior-posterior axis. Developmental cell *20*, 19-32.

Cacchiarelli, D., Incitti, T., Martone, J., Cesana, M., Cazzella, V., Santini, T., Sthandier, O., and Bozzoni, I. (2011). miR-31 modulates dystrophin expression: new implications for Duchenne muscular dystrophy therapy. EMBO reports *12*, 136-141.

Cai, C., Coleman, S.K., Niemi, K., and Keinänen, K. (2002). Selective binding of synapse-associated protein 97 to GluR-A α-amino-5-hydroxy-3-methyl-4-isoxazole propionate receptor subunit is determined by a novel sequence motif. Journal of Biological Chemistry *277*, 31484-31490.

Choi, J.-H., Yu, N.-K., Baek, G.-C., Bakes, J., Seo, D., Nam, H.J., Baek, S.H., Lim, C.-S., Lee, Y.-S., and Kaang, B.-K. (2014). Optimization of AAV expression cassettes to improve packaging capacity and transgene expression in neurons. Mol brain *7*, 1-10.

Cogswell, J.P., Ward, J., Taylor, I.A., Waters, M., Shi, Y., Cannon, B., Kelnar, K., Kemppainen, J., Brown, D., and Chen, C. (2008). Identification of miRNA changes in Alzheimer's disease brain and CSF yields putative biomarkers and insights into disease pathways. Journal of Alzheimer's disease *14*, 27-41.

Collingridge, G., Kehl, S., and McLennan, H.t. (1983). Excitatory amino acids in synaptic transmission in the Schaffer collateral-commissural pathway of the rat hippocampus. The Journal of physiology *334*, 33-46.

Coolen, M., Katz, S., and Bally-Cuif, L. (2015). miR-9: a versatile regulator of neurogenesis. Regulatory RNAs in the Nervous System.

Coolen, M., Thieffry, D., Drivenes, Ø ., Becker, T.S., and Bally-Cuif, L. (2012). miR-9 controls the timing of neurogenesis through the direct inhibition of antagonistic factors. Developmental cell *22*, 1052-1064.

Dajas-Bailador, F., Bonev, B., Garcez, P., Stanley, P., Guillemot, F., and Papalopulu,

N. (2012). microRNA-9 regulates axon extension and branching by targeting Map1b in mouse cortical neurons. Nature neuroscience *15*, 697-699.

Delaloy, C., Liu, L., Lee, J.-A., Su, H., Shen, F., Yang, G.-Y., Young, W.L., Ivey, K.N., and Gao, F.-B. (2010). MicroRNA-9 coordinates proliferation and migration of human embryonic stem cell-derived neural progenitors. Cell Stem Cell *6*, 323-335.

Denli, A.M., Tops, B.B., Plasterk, R.H., Ketting, R.F., and Hannon, G.J. (2004). Processing of primary microRNAs by the Microprocessor complex. Nature *432*, 231-235.

Doench, J.G., and Sharp, P.A. (2004). Specificity of microRNA target selection in translational repression. Genes & development *18*, 504-511.

Ebert, M.S., Neilson, J.R., and Sharp, P.A. (2007). MicroRNA sponges: competitive inhibitors of small RNAs in mammalian cells. Nature methods *4*, 721-726.

Emery, A.E. (1991). Population frequencies of inherited neuromuscular diseases—a world survey. Neuromuscular disorders *1*, 19-29.

Friedman, R.C., Farh, K.K.-H., Burge, C.B., and Bartel, D.P. (2009). Most mammalian mRNAs are conserved targets of microRNAs. Genome research *19*, 92-105.

Gao, J., Wang, W.-Y., Mao, Y.-W., Gräff, J., Guan, J.-S., Pan, L., Mak, G., Kim, D., Su, S.C., and Tsai, L.-H. (2010). A novel pathway regulates memory and plasticity via SIRT1 and miR-134. Nature *466*, 1105-1109.

Garcia, D.M., Baek, D., Shin, C., Bell, G.W., Grimson, A., and Bartel, D.P. (2011). Weak seed-pairing stability and high target-site abundance decrease the proficiency of lsy-6 and other microRNAs. Nature structural & molecular biology *18*, 1139-1146.

Giese, K.P., Fedorov, N.B., Filipkowski, R.K., and Silva, A.J. (1998). Autophosphorylation at Thr286 of the α calcium-calmodulin kinase II in LTP and learning. Science *279*, 870-873.

Giusti, S.A., Vogl, A.M., Brockmann, M.M., Vercelli, C.A., Rein, M.L., Trumbach, D., Wurst, W., Cazalla, D., Stein, V., Deussing, J.M., *et al.* (2014). MicroRNA-9 controls dendritic development by targeting REST. eLife *3*.

Griffiths-Jones, S., Saini, H.K., van Dongen, S., and Enright, A.J. (2008). miRBase: tools for microRNA genomics. Nucleic acids research *36*, D154-D158.

Grimson, A., Farh, K.K.-H., Johnston, W.K., Garrett-Engele, P., Lim, L.P., and Bartel, D.P. (2007). MicroRNA targeting specificity in mammals: determinants beyond seed pairing. Molecular cell *27*, 91-105.

Hébert, S.S., Horré, K., Nicolaï, L., Papadopoulou, A.S., Mandemakers, W., Silahtaroglu, A.N., Kauppinen, S., Delacourte, A., and De Strooper, B. (2008). Loss of microRNA cluster miR-29a/b-1 in sporadic Alzheimer's disease correlates with increased BACE1/β-secretase expression. Proceedings of the National Academy of Sciences *105*, 6415-6420.

Han, J., Lee, Y., Yeom, K.-H., Kim, Y.-K., Jin, H., and Kim, V.N. (2004). The Drosha-DGCR8 complex in primary microRNA processing. Genes & development *18*, 3016-3027.

He, L., and Hannon, G.J. (2004). MicroRNAs: small RNAs with a big role in gene regulation. Nature Reviews Genetics *5*, 522-531.

He, M., Liu, Y., Wang, X., Zhang, M.Q., Hannon, G.J., and Huang, Z.J. (2012). Cell-type-based analysis of microRNA profiles in the mouse brain. Neuron *73*, 35-48.

Hoffman, E.P., Brown Jr, R.H., and Kunkel, L.M. (1987). Dystrophin: the protein

product of the Duchenne muscular dystrophy locus. Cell *51*, 919-928.

Howard, M.A., Elias, G.M., Elias, L.A., Swat, W., and Nicoll, R.A. (2010). The role of SAP97 in synaptic glutamate receptor dynamics. Proceedings of the National Academy of Sciences *107*, 3805-3810.

Huerta, P.T., Sun, L.D., Wilson, M.A., and Tonegawa, S. (2000). Formation of temporal memory requires NMDA receptors within CA1 pyramidal neurons. Neuron *25*, 473-480.

John, B., Enright, A.J., Aravin, A., Tuschl, T., Sander, C., and Marks, D.S. (2004). Human microRNA targets. PLoS Biol *2*, e363.

Kandel, E.R. (2012). The molecular biology of memory: cAMP, PKA, CRE, CREB-1, CREB-2, and CPEB. Mol Brain *5*, 14.

Kapsimali, M., Kloosterman, W.P., De Bruijn, E., Rosa, F., Plasterk, R., and Wilson, S.W. (2007). MicroRNAs show a wide diversity of expression profiles in the developing and mature central nervous system. Genome Biol *8*, R173.

Kent, W.J., Sugnet, C.W., Furey, T.S., Roskin, K.M., Pringle, T.H., Zahler, A.M., and Haussler, D. (2002). The human genome browser at UCSC. Genome research *12*, 996-1006.

Kertesz, M., Iovino, N., Unnerstall, U., Gaul, U., and Segal, E. (2007). The role of site accessibility in microRNA target recognition. Nature genetics *39*, 1278-1284.

Kim, M., Huang, T., Abel, T., and Blackwell, K.T. (2010). Temporal sensitivity of protein kinase a activation in late-phase long term potentiation. PLoS Comput Biol *6*, e1000691.

Kim, T.-W., Wu, K., Xu, J.-l., and Black, I.B. (1992). Detection of dystrophin in the postsynaptic density of rat brain and deficiency in a mouse model of Duchenne

muscular dystrophy. Proceedings of the National Academy of Sciences *89*, 11642-11644.

Klein, M.E., Lioy, D.T., Ma, L., Impey, S., Mandel, G., and Goodman, R.H. (2007). Homeostatic regulation of MeCP2 expression by a CREB-induced microRNA. Nature neuroscience *10*.

Kloosterman, W.P., Wienholds, E., de Bruijn, E., Kauppinen, S., and Plasterk, R.H. (2006). In situ detection of miRNAs in animal embryos using LNA-modified oligonucleotide probes. Nature methods *3*, 27-29.

Konopka, W., Kiryk, A., Novak, M., Herwerth, M., Parkitna, J.R., Wawrzyniak, M., Kowarsch, A., Michaluk, P., Dzwonek, J., and Arnsperger, T. (2010). MicroRNA loss enhances learning and memory in mice. The Journal of neuroscience *30*, 14835-14842.

Kozomara, A., and Griffiths-Jones, S. (2014). miRBase: annotating high confidence microRNAs using deep sequencing data. Nucleic acids research *42*, D68-D73.

Krek, A., Grün, D., Poy, M.N., Wolf, R., Rosenberg, L., Epstein, E.J., MacMenamin, P., da Piedade, I., Gunsalus, K.C., and Stoffel, M. (2005). Combinatorial microRNA target predictions. Nature genetics *37*, 495-500.

Krichevsky, A.M., Sonntag, K.C., Isacson, O., and Kosik, K.S. (2006). Specific microRNAs modulate embryonic stem cell–derived neurogenesis. Stem cells *24*, 857-864.

Lagos-Quintana, M., Rauhut, R., Lendeckel, W., and Tuschl, T. (2001). Identification of novel genes coding for small expressed RNAs. Science *294*, 853-858.

Lagos-Quintana, M., Rauhut, R., Yalcin, A., Meyer, J., Lendeckel, W., and Tuschl,

T. (2002). Identification of tissue-specific microRNAs from mouse. Current Biology *12*, 735-739.

Lai, E.C., Wiel, C., and Rubin, G.M. (2004). Complementary miRNA pairs suggest a regulatory role for miRNA: miRNA duplexes. Rna *10*, 171-175.

Landgraf, P., Rusu, M., Sheridan, R., Sewer, A., Iovino, N., Aravin, A., Pfeffer, S., Rice, A., Kamphorst, A.O., and Landthaler, M. (2007). A mammalian microRNA expression atlas based on small RNA library sequencing. Cell *129*, 1401-1414.

Lau, N.C., Lim, L.P., Weinstein, E.G., and Bartel, D.P. (2001). An abundant class of tiny RNAs with probable regulatory roles in Caenorhabditis elegans. Science *294*, 858-862.

Lee, R.C., and Ambros, V. (2001). An extensive class of small RNAs in Caenorhabditis elegans. Science *294*, 862-864.

Lee, R.C., Feinbaum, R.L., and Ambros, V. (1993). The C. elegans heterochronic gene lin-4 encodes small RNAs with antisense complementarity to lin-14. Cell *75*, 843-854.

Lee, Y.-S., Ehninger, D., Zhou, M., Oh, J.-Y., Kang, M., Kwak, C., Ryu, H.-H., Butz, D., Araki, T., and Cai, Y. (2014). Mechanism and treatment for learning and memory deficits in mouse models of Noonan syndrome. Nature neuroscience *17*, 1736-1743.

Lee, Y., Ahn, C., Han, J., Choi, H., Kim, J., Yim, J., Lee, J., Provost, P., Rådmark, O., and Kim, S. (2003). The nuclear RNase III Drosha initiates microRNA processing. nature *425*, 415-419.

Lee, Y., Jeon, K., Lee, J.T., Kim, S., and Kim, V.N. (2002). MicroRNA maturation: stepwise processing and subcellular localization. The EMBO journal *21*, 4663-4670.

Lee, Y., Kim, M., Han, J., Yeom, K.H., Lee, S., Baek, S.H., and Kim, V.N. (2004).

MicroRNA genes are transcribed by RNA polymerase II. The EMBO journal *23*, 4051-4060.

Leonard, A.S., Davare, M.A., Horne, M., Garner, C.C., and Hell, J.W. (1998). SAP97 is associated with the α-amino-3-hydroxy-5-methylisoxazole-4-propionic acid receptor GluR1 subunit. Journal of Biological Chemistry *273*, 19518-19524.

Leucht, C., Stigloher, C., Wizenmann, A., Klafke, R., Folchert, A., and Bally-Cuif, L. (2008). MicroRNA-9 directs late organizer activity of the midbrain-hindbrain boundary. Nature neuroscience *11*, 641-648.

Lewis, B.P., Burge, C.B., and Bartel, D.P. (2005). Conserved seed pairing, often flanked by adenosines, indicates that thousands of human genes are microRNA targets. cell *120*, 15-20.

Lewis, B.P., Shih, I.-h., Jones-Rhoades, M.W., Bartel, D.P., and Burge, C.B. (2003). Prediction of mammalian microRNA targets. Cell *115*, 787-798.

Li, D., Specht, C.G., Waites, C.L., Butler-Munro, C., Leal-Ortiz, S., Foote, J.W., Genoux, D., Garner, C.C., and Montgomery, J.M. (2011). SAP97 directs NMDA receptor spine targeting and synaptic plasticity. The Journal of physiology *589*, 4491-4510.

Lidov, H.G., Byers, T.J., Watkins, S.C., and Kunkel, L.M. (1990). Localization of dystrophin to postsynaptic regions of central nervous system cortical neurons. Nature *348*, 725-728.

Lim, C.-S., Hoang, E.T., Viar, K.E., Stornetta, R.L., Scott, M.M., and Zhu, J.J. (2014). Pharmacological rescue of Ras signaling, GluA1-dependent synaptic plasticity, and learning deficits in a fragile X model. Genes & development *28*, 273-289.

Liu, D.Z., Ander, B.P., Tian, Y., Stamova, B., Jickling, G.C., Davis, R.R., and Sharp, F.R. (2012). Integrated analysis of mRNA and microRNA expression in mature neurons, neural progenitor cells and neuroblastoma cells. Gene *495*, 120-127.

Loya, C.M., Lu, C.S., Van Vactor, D., and Fulga, T.A. (2009). Transgenic microRNA inhibition with spatiotemporal specificity in intact organisms. Nature methods *6*, 897-903.

Lynch, M. (2004). Long-term potentiation and memory. Physiological reviews *84*, 87-136.

Malinow, R., and Malenka, R.C. (2002). AMPA receptor trafficking and synaptic plasticity. Annual review of neuroscience *25*, 103-126.

Martin, S., Grimwood, P., and Morris, R. (2000). Synaptic plasticity and memory: an evaluation of the hypothesis. Annual review of neuroscience *23*, 649-711.

Martinez, J., and Tuschl, T. (2004). RISC is a 5′ phosphomonoester-producing RNA endonuclease. Genes & development *18*, 975-980.

Meister, G., Landthaler, M., Dorsett, Y., and Tuschl, T. (2004). Sequence-specific inhibition of microRNA-and siRNA-induced RNA silencing. Rna *10*, 544-550.

Mellios, N., Sugihara, H., Castro, J., Banerjee, A., Le, C., Kumar, A., Crawford, B., Strathmann, J., Tropea, D., and Levine, S.S. (2011). miR-132, an experience-dependent microRNA, is essential for visual cortex plasticity. Nature neuroscience *14*, 1240-1242.

Milner, B., Squire, L.R., and Kandel, E.R. (1998). Cognitive neuroscience and the study of memory. Neuron *20*, 445-468.

Miska, E.A., Alvarez-Saavedra, E., Townsend, M., Yoshii, A., Šestan, N., Rakic, P., Constantine-Paton, M., and Horvitz, H.R. (2004). Microarray analysis of microRNA

expression in the developing mammalian brain. Genome biology *5*, R68.

Morris, R., Garrud, P., Rawlins, J., and O'Keefe, J. (1982). Place navigation impaired in rats with hippocampal lesions. Nature *297*, 24.

Muntoni, F., Mateddu, A., and Serra, G. (1991). Passive avoidance behaviour deficit in the *mdx* mouse. Neuromuscular Disorders *1*, 121-123.

Nakagawa, T., Futai, K., Lashuel, H.A., Lo, I., Okamoto, K., Walz, T., Hayashi, Y., and Sheng, M. (2004a). Quaternary structure, protein dynamics, and synaptic function of SAP97 controlled by L27 domain interactions. Neuron *44*, 453-467.

Nakagawa, T., Futai, K., Lashuel, H.A., Lo, I., Okamoto, K., Walz, T., Hayashi, Y., and Sheng, M. (2004b). Quaternary structure, protein dynamics, and synaptic function of SAP97 controlled by L27 domain interactions. Neuron *44*, 453-467.

Nash, J.E., Appleby, V.J., Corrêa, S.A., Wu, H., Fitzjohn, S.M., Garner, C.C., Collingridge, G.L., and Molnár, E. (2010). Disruption of the interaction between myosin VI and SAP97 is associated with a reduction in the number of AMPARs at hippocampal synapses. Journal of neurochemistry *112*, 677-690.

O'Keefe, J., and Dostrovsky, J. (1971). The hippocampus as a spatial map. Preliminary evidence from unit activity in the freely-moving rat. Brain research *34*, 171-175.

Oliveira, A.M., Hawk, J.D., Abel, T., and Havekes, R. (2010). Post-training reversible inactivation of the hippocampus enhances novel object recognition memory. Learning & Memory *17*, 155-160.

Otaegi, G., Pollock, A., Hong, J., and Sun, T. (2011). MicroRNA miR-9 modifies motor neuron columns by a tuning regulation of FoxP1 levels in developing spinal cords. The Journal of Neuroscience *31*, 809-818.

Packer, A.N., Xing, Y., Harper, S.Q., Jones, L., and Davidson, B.L. (2008). The bifunctional microRNA miR-9/miR-9* regulates REST and CoREST and is downregulated in Huntington's disease. The Journal of Neuroscience *28*, 14341-14346.

Park, P., Sanderson, T.M., Amici, M., Choi, S.-L., Bortolotto, Z.A., Zhuo, M., Kaang, B.-K., and Collingridge, G.L. (2016). Calcium-Permeable AMPA Receptors Mediate the Induction of the Protein Kinase A-Dependent Component of Long-Term Potentiation in the Hippocampus. The Journal of Neuroscience *36*, 622-631.

Park, P., Volianskis, A., Sanderson, T.M., Bortolotto, Z.A., Jane, D.E., Zhuo, M., Kaang, B.-K., and Collingridge, G.L. (2014). NMDA receptor-dependent long-term potentiation comprises a family of temporally overlapping forms of synaptic plasticity that are induced by different patterns of stimulation. Phil Trans R Soc B *369*, 20130131.

Rajasethupathy, P., Fiumara, F., Sheridan, R., Betel, D., Puthanveettil, S.V., Russo, J.J., Sander, C., Tuschl, T., and Kandel, E. (2009). Characterization of Small RNAs in< i> Aplysia</i> Reveals a Role for miR-124 in Constraining Synaptic Plasticity through CREB. Neuron *63*, 803-817.

Reinhart, B.J., Slack, F.J., Basson, M., Pasquinelli, A.E., Bettinger, J.C., Rougvie, A.E., Horvitz, H.R., and Ruvkun, G. (2000). The 21-nucleotide let-7 RNA regulates developmental timing in Caenorhabditis elegans. nature *403*, 901-906.

Rumbaugh, G., Sia, G.-M., Garner, C.C., and Huganir, R.L. (2003). Synapse-associated protein-97 isoform-specific regulation of surface AMPA receptors and synaptic function in cultured neurons. The Journal of neuroscience *23*, 4567-4576.

Schlüter, O.M., Xu, W., and Malenka, R.C. (2006). Alternative N-terminal domains

of PSD-95 and SAP97 govern activity-dependent regulation of synaptic AMPA receptor function. Neuron *51*, 99-111.

Schnell, E., Sizemore, M., Karimzadegan, S., Chen, L., Bredt, D.S., and Nicoll, R.A. (2002). Direct interactions between PSD-95 and stargazin control synaptic AMPA receptor number. Proceedings of the National Academy of Sciences *99*, 13902-13907.

Schratt, G. (2009). microRNAs at the synapse. Nature Reviews Neuroscience *10*, 842-849.

Schratt, G.M., Tuebing, F., Nigh, E.A., Kane, C.G., Sabatini, M.E., Kiebler, M., and Greenberg, M.E. (2006). A brain-specific microRNA regulates dendritic spine development. Nature *439*, 283-289.

Schwarz, D.S., Hutvágner, G., Du, T., Xu, Z., Aronin, N., and Zamore, P.D. (2003). Asymmetry in the assembly of the RNAi enzyme complex. Cell *115*, 199-208.

Scoville, W.B., and Milner, B. (1957). Loss of recent memory after bilateral hippocampal lesions. Journal of neurology, neurosurgery, and psychiatry *20*, 11.

Sempere, L.F., Freemantle, S., Pitha-Rowe, I., Moss, E., Dmitrovsky, E., and Ambros, V. (2004). Expression profiling of mammalian microRNAs uncovers a subset of brain-expressed microRNAs with possible roles in murine and human neuronal differentiation. Genome biology *5*, R13.

Shibata, M., Nakao, H., Kiyonari, H., Abe, T., and Aizawa, S. (2011). MicroRNA-9 regulates neurogenesis in mouse telencephalon by targeting multiple transcription factors. The Journal of Neuroscience *31*, 3407-3422.

Sicinski, P., Geng, Y., Ryder-Cook, A.S., Barnard, E.A., Darlison, M.G., and Barnard, P.J. (1989). The molecular basis of muscular dystrophy in the mdx mouse: a point

mutation. Science *244*, 1578-1580.

Sutton, M.A., and Schuman, E.M. (2006). Dendritic protein synthesis, synaptic plasticity, and memory. Cell *127*, 49-58.

Tennyson, C.N., Klamut, H.J., and Worton, R.G. (1995). The human dystrophin gene requires 16 hours to be transcribed and is cotranscriptionally spliced. Nature genetics *9*, 184-190.

Tognini, P., Putignano, E., Coatti, A., and Pizzorusso, T. (2011). Experience-dependent expression of miR-132 regulates ocular dominance plasticity. Nature neuroscience *14*, 1237-1239.

Tsien, J.Z., Huerta, P.T., and Tonegawa, S. (1996). The essential role of hippocampal CA1 NMDA receptor–dependent synaptic plasticity in spatial memory. Cell *87*, 1327-1338.

Vaillend, C., Billard, J.-M., and Laroche, S. (2004a). Impaired long-term spatial and recognition memory and enhanced CA1 hippocampal LTP in the dystrophin-deficient *Dmd*^{mdx} mouse. Neurobiology of disease *17*, 10-20.

Vaillend, C., Billard, J.-M., and Laroche, S. (2004b). Impaired long-term spatial and recognition memory and enhanced CA1 hippocampal LTP in the dystrophin-deficient< i> Dmd</i>< sup> mdx</sup> mouse. Neurobiology of disease *17*, 10-20.

Vaillend, C., Rendon, A., Misslin, R., and Ungerer, A. (1995). Influence of dystrophin-gene mutation onmdx mouse behavior. I. Retention deficits at long delays in spontaneous alternation and bar-pressing tasks. Behavior genetics *25*, 569-579.

Vaillend, C., Ungerer, A., and Billard, J.M. (1999). Facilitated NMDA receptor-

mediated synaptic plasticity in the hippocampal CA1 area of dystrophin-deficient mice. Synapse *33*, 59-70.

Vester, B., and Wengel, J. (2004). LNA (locked nucleic acid): high-affinity targeting of complementary RNA and DNA. Biochemistry *43*, 13233-13241.

Waites, C.L., Specht, C.G., Härtel, K., Leal-Ortiz, S., Genoux, D., Li, D., Drisdel, R.C., Jeyifous, O., Cheyne, J.E., and Green, W.N. (2009). Synaptic SAP97 isoforms regulate AMPA receptor dynamics and access to presynaptic glutamate. The Journal of neuroscience *29*, 4332-4345.

Wei, X., Li, H., Miao, J., Liu, B., Zhan, Y., Wu, D., Zhang, Y., Wang, L., Fan, Y., and Gu, H. (2013). miR-9*-and miR-124a-Mediated switching of chromatin remodelling complexes is altered in rat spina bifida aperta. Neurochemical research *38*, 1605-1615.

Wheeler, B.M., Heimberg, A.M., Moy, V.N., Sperling, E.A., Holstein, T.W., Heber, S., and Peterson, K.J. (2009). The deep evolution of metazoan microRNAs. Evolution & development *11*, 50-68.

Wightman, B., Ha, I., and Ruvkun, G. (1993). Posttranscriptional regulation of the heterochronic gene lin-14 by lin-4 mediates temporal pattern formation in C. elegans. Cell *75*, 855-862.

Woo, N.H., Duffy, S.N., Abel, T., and Nguyen, P.V. (2003). Temporal spacing of synaptic stimulation critically modulates the dependence of LTP on cyclic AMP-dependent protein kinase. Hippocampus *13*, 293-300.

Yi, R., Qin, Y., Macara, I.G., and Cullen, B.R. (2003). Exportin-5 mediates the nuclear export of pre-microRNAs and short hairpin RNAs. Genes & development *17*, 3011-3016.

Yoo, A.S., Staahl, B.T., Chen, L., and Crabtree, G.R. (2009). MicroRNA-mediated switching of chromatin-remodelling complexes in neural development. Nature *460*, 642-646.

Yoo, A.S., Sun, A.X., Li, L., Shcheglovitov, A., Portmann, T., Li, Y., Lee-Messer, C., Dolmetsch, R.E., Tsien, R.W., and Crabtree, G.R. (2011). MicroRNA-mediated conversion of human fibroblasts to neurons. Nature *476*, 228-231.

Yuva-Aydemir, Y., Simkin, A., Gascon, E., and Gao, F.-B. (2011). MicroRNA-9. RNA biology *8*, 557-564.

Zhao, C., Sun, G., Li, S., and Shi, Y. (2009). A feedback regulatory loop involving microRNA-9 and nuclear receptor TLX in neural stem cell fate determination. Nature structural & molecular biology *16*, 365-371.

Zhao, M.-G., Toyoda, H., Ko, S.W., Ding, H.-K., Wu, L.-J., and Zhuo, M. (2005). Deficits in trace fear memory and long-term potentiation in a mouse model for fragile X syndrome. The Journal of neuroscience *25*, 7385-7392.

국문초록

microRNA는 단백질을 합성하지 않는 작은 RNA (~22개 뉴클레오타이드)로서, 여러 조직에서 유전자의 전사후 발현을 조절한다. microRNA를 통한 전사 후 유전자 조절은 시냅스 가소성과 기억을 포함한 생리학적 뇌기능에 필수적인 역할을 한다고 알려져 있다. 지금까지 많은 뇌 특이적 microRNA들이 확인되었지만, 그 중 몇몇 microRNA만이 학습과 기억을 조절한다고 알려져 있다. miR-9-5p/3p는 진화적으로 보존된 뇌 특이적인 microRNA로서 발달을 조절한다고 알려져 있고, 몇몇 신경성 질병에서 중요성이 제기되고 있지만 아직 성숙신경세포에서의 역할은 아직 밝혀진 바가 없다. 이 연구에서는 뇌 특이적인 microRNA인 miR-9-3p (또는 miR-9*)의 해마 시냅스 가소성과 기억에서의 기능을 microRNA 스폰지라는 microRNA의 경쟁적 억제자를 사용해 밝혔다. miR-9-3p를 억제하였을 때, 해마 시냅스의 장기강화가 감손된다는 것을 홀셀레코딩 실험기법을 통해 보였다. miR-9-3p의 억제는 기본 시냅스 전달과 막 흥분성에는 영향이 없었다. 반면, miR-9-3p의 상보적인 microRNA인 miR-9-5p는 해마 시냅스의 장기강화에 영향이 없었다. 또한 miR-9-3p를 해마에서 억제하였을 때, 생쥐의 해마 의존적인 학습과 기억이 손상된 것을 확인하였다. 이는 세 가지 해마 의존 행동실험인 모리스 수중 미로, 물체 위치 기억, 트레이스 공포 검사 모두에서 나타났다. 이러한 결과들은 miR-9-3p를 통한 조절이 해

마에서의 시냅스 가소성과 기억에 중요한 역할을 한다는 것을 시사한다. 뿐만 아니라, 일련의 생물정보학적 분석과 광범위한 기존의 연구 결과들을 통해 miR-9-3p의 조절 대상이라고 생각되는 7개의 후보 유전자를 찾았고, 실제로 이들 후보 유전자들의 발현이 miR-9-3p에 의해 조절된다는 것을 확인하였다. 마지막으로, miR-9-3p를 억제하였을 때, 후보 유전자들 중 Dmd와 SAP97의 단백질이 증가한다는 것을 발견하였고, 이는 miR-9-3p의 분자적 작용 메커니즘으로 생각된다.

요약하면, miR-9-3p는 해마의 시냅스 장기강화와 기억에 중요한 역할을 하고 있으며, 이는 *Dmd*와 *SAP97* 유전자를 조절함으로써 작용한다. 이 연구는 miR-9-3p가 시냅스 가소성과 기억에 중요한 역할을 한다는 처음으로 제시한다.

.....

주요어: microRNA, miR-9-5p/3p, 해마, 시냅스 가소성, 기억